A

Thesis

on

Development of a photo oxidation/reduction electrode in photocatalytic study

Submitted By

Pallav Nayak

(710CH1022)

Under the Supervision of

Dr. Pradip Chowdhury

In partial fulfillment for the award of the degree of

Master of Technology (Dual Degree)
in
Chemical Engineering

DEPARTMENT OF CHEMICAL ENGINEERING

NATIONAL INSTITUTE OF TECHNOLOGY ROURKELA

MAY, 2015

Certificate

Certified that work presented in this thesis entitled ***"Development of a photo oxidation/reduction electrode in photocatalytic study"*** *by* ***Pallav Nayak (710CH1022)*** *has been carried out under my supervision and this work has not been submitted elsewhere for a degree.*

Date: 25-05-2015

_____

(Thesis Supervisor)

Dr. Pradip Chowdhury
Assistant Professor
Department of Chemical Engineering
National Institute of Technology, Rourkela

ACKNOWLEDGEMENTS

First and the foremost, I take this opportunity my express my profound sense of gratitude to my thesis supervisor **Dr. Pradip Chowdhury** for his colossal interest and enthusiasm on the project. His technical expertise and immense understanding on diverse fields left quite an impression on me. He was always welcome to new ideas and worked for hours with me. Despite the fact that the journey was assailed with complexities however I always discovered his help and support. He has been a steady wellspring of motivation for me.

I am also thankful to the HOD, faculties and support staff of Department of Chemical Engineering, National Institute of Technology Rourkela, for their constant help and extending the departmental facilities for carrying out my project work.

I also got great support from many technical assistants of various other departments *viz*. Metallurgical and Material Science Engineering, Physics, Chemistry and Ceramic Engineering during the course of my work. I greatly acknowledge their contribution.

I also sincerely extend my thankfulness to all the members of our research group particularly Prince George and Santosh Hippale for their help. I would also cherish the help and encouragement by my friends and colleagues.

Last but not the least I would also like to thank my beloved parents for their encouragement in every sphere of my life. I always found their healing touch whenever I had a rough patch in my life and I owe everything to them.

Date: 25th May, 2015 **Pallav Nayak**

Place: Rourkela

To

My Parents and Teachers

ABSTRACT

Catalysis has been a thrust area in materials research and MOFs have shown potential to make strong in-road in catalytic applications. Many of these MOFs reportedly have shown photo-sensitivity and since photocatalysis constitute one of the most intriguing areas of research within the domain of catalysis, it would be worth an effort to probe their effectiveness as photocatalyst. Although, the success or failure of any MOF compound as photocatalyst would largely depend on their ability to remain stable under aqueous and/or organic medium on prolonged exposure. Transparent conducting oxide (TCO) thin film is a recent concept. High transparency and low electrical resistivity (in the visible wavelength region) are some of its key features. Harnessing solar energy has been a thrust area and gaining momentum continually. Various methods, products and technologies have been developed towards this direction and our present research endeavor and motivation is mainly sourced from the issue on harnessing solar energy in photo degradation. In this work, two contemporary metal organic frameworks (MOFs) i.e. MOF-5 (Zn-BDC) and MIL-53(Fe) (or, Fe-BDC) were synthesized using *microwave synthesis* technique and characterized. Owing to their photo-sensitivity, both the MOFs were used in photo-degradation of ammonia. The results were compared with the performance of a standard photocatalyst *viz*. ZnO. Transparent conducting oxide (TCO) thin films were fabricated by sol-gel and spin coating techniques. MOF films (Zn-BDC) were grown onto TCO. Improvisations were also made in TCO matrix by using Al and Pb as doping agents. The doping percentage as well as the number of cycles of coating was varied so as to get the most suitable TCO. The films were characterized using X-ray diffraction, Scanning electron microscopy, UV-reflectance and UV-transmittance (by spectrophotometer) study. The band gap calculations for the films were measured from the UV-reflectance data which showed the band gap value of nearly 3.2 eV. The performance study of MOFs and ZnO as photocatalyst were carried out in degradation of ammonia. When used directly, MOFs had shown a better degradation percentage (*ca*. 60%) as compared to ZnO and that could be attributed to their very high specific surface area as compared to ZnO. Meanwhile, TCO films of various combinations when tested for their electrical conductivity are met with limited success and further work is going on towards achieving the targeted results.

Keywords: Metal organic frameworks, Transparent conducting oxides, Sol-Gel technique, spin coating, photocatalysis.

TABLE OF CONTENTS

LIST OF FIGURES

LIST OF TABLES

ABBREVIATIONS

BET	-	Brunauer, Emmett and Teller
BDC	-	Benzene dicarboxylic acid
DMF	-	Dimethyl Formamide
EDX	-	Energy Dispersive X-Ray Spectroscopy
EM	-	Electromagnetic Spectrum
MIL	-	MatérialInstitute Lavoisier
MOF	-	Metal Organic Framework
TCO	-	Transparent Conducting Oxides
PXRD	-	Powder X-Ray Diffraction
SBU	-	Secondary Building Units
SEM	-	Scanning Electron Microscope
TGA	-	Thermo Gravimetric Analysis
UV	-	Ultraviolet

CHAPTER 1

INTRODUCTION

Technology is the beacon of development. New materials give rise to newer technology. Synthesizing and integrating novel materials has always been esteemed as a venturing stone in technological advancement. Bringing metal organic frameworks and transparent conducting oxide films together to develop a photo electrode is a fresh field of research that can modernize photo catalysis technology.

1.1 Prelude

Lately, researchers have made quick and huge advances in the field of material science, particularly in semiconductor material science. A standout amongst the most vital fields of the current enthusiasm for materials science is the principal perspectives and utilizations of conducting transparent oxide thin films (TCO). Having characteristic property of high transparency and low electrical resistivity, they can be used for substantial technological advancement. MOFs have also been a very keen area of research for the past decade because of their high surface area and pore volume. Proper selection of inorganic metal atoms/ions and organic ligands lead to an array of possibilities in topology and functionalities within MOFs. Additionally embedding metal organic frameworks (MOFs) on the TCO will make highly advanced photoelectrode which can have potential applications in photocatalysis.

1.2 Background of research

Metal Organic Frameworks (or, MOFs) are fundamentally known for their versatility in structural architecture. Proper selection of inorganic metal atoms/ions and organic ligands lead to an array of possibilities in topology and functionalities within MOFs. Extraordinary specific surface area (*ca*. 100-5500 m^2 g^{-1}) and pore volume (*ca*. 0.5-3.5 ml g^{-1}), uniform pore size distribution, tunable or tailor-made matrices, product purity, variety in functionality and aperture size/shape are some of the key features of this class of materials. The salient features of MOFs

have attracted wide attention within the research community ever since its inception and found applications in areas ranging from *adsorptive gas separation/purification, energy storage, catalysis, drug delivery, sensors* etc.

Catalysis has been a thrust area in materials research and MOFs have shown potential to make strong in-road in catalytic applications. Many of these MOFs reportedly have shown photo-sensitivity and since photocatalysis constitute one of the most intriguing areas of research within the domain of catalysis, it would be worth an effort to probe their effectiveness as photocatalyst. Although, the success or failure of any MOF compound as photocatalyst would largely depend on their ability to remain stable under aqueous and/or organic medium on prolonged exposure, especially, since only a select few of them have surpassed the benchmark stability standard.

Transparent conducting oxide (TCO) thin film is a recent concept. High transparency and low electrical resistivity (in the visible wavelength region) are some of its key features. These conducting transparent films have already been used in a variety of interesting applications such as gas sensors, solar cells, heat reflectors, protective coatings, light transparent electrodes and laser damage resistant coatings in high power laser technology.

Harnessing solar energy has been a thrust area and gaining momentum continually. Various methods, products and technologies have been developed towards this direction and our present research endeavour and motivation is mainly sourced from the issue on harnessing solar energy in photo degradation.

1.3 Research objectives

The aim and scope of this work can be summarized as:

(i) Synthesis and characterization of contemporary metal organic frameworks using microwave technique.

(ii) Evaluating their photo-sensitivity for their application in photocatalysis.

(iii) Photo-degradation of ammonia using MOFs as photocatalysts and comparing data with the performance of standard ZnO photocatalyst.

(iv) Fabrication of transparent conducting oxide (TCO) thin films and growing MOF onto it and improvisation of surface characteristics by various suitable doping agents.

(v) Characterization of TCO for developing into a photo-electrode.

1.4 Thesis Summary

The complete thesis has been arranged into five chapters. **Chapter 1** (Introduction) defines the basic chemistry of metal organic frameworks and transparent conducting oxides. It also explains the background of the present work and highlights the objectives. **Chapter 2** (Literature review) illustrates the structural chemistry of MOFs and TCOs. Advances on catalysis with special emphasis on photocatalysis and ammonia degradation are also narrated. **Chapter 3** (Experimental works) explains the systematic investigation on material synthesis and their characterization. Detail protocols followed during photocatalytic applications and ammonia degradation analysis using MOFs are also documented in this section. **Chapter 4** (Results and discussion) gives proper reasoning on all experimental results with appropriate references, systematically. **Chapter 5** (Conclusion and future scope) concludes the research findings in a point by point manner. The future scope or extension of this present research work is also highlighted in this section.

CHAPTER 2

LITERATURE SURVEY

In the following paragraphs the details on photoconductivity and photocatalysts have been discussed along with highlighted breakthrough research. The definition and structural features of MOFs along with its synthesis procedures and myriad different application potentials with special emphasis on photocatalysis are discussed as well. The fundamental concepts of Transparent Conducting Oxides (TCO) and various experimental methodologies to develop TCOs are discussed as well with ZnO as an example. Finally, developing Zn-BDC or MOF-5 into a potential TCO has been stressed upon and basic work done by other research groups is highlighted.

2.1 Photoconductivity Studies

Throughout the previous two decades, it was surely understood that the photo response of n-type metal oxide semiconductors, such as zinc oxides and titanium oxides exhibited slow conduction decay process, which was controlled by surface effects such as gas absorption and desorption. In the absence of light, oxygen gas adsorbed on the oxide surface as a negatively charged ion by taking free electrons of the n-type oxide semiconductors, created a depletion layer, with lesser conductivity close to the film surface. When this was illuminated, holes formed by absorption of light close to the film surface, migrated to the surface due to the band bending and discharged the negatively charged adsorbed oxygen ions. The electrons formed simultaneously, by the light, destructed the depletion layer, increasing the conductivity. Thus the photo response in ZnO included adsorption and photo desorption of oxygen on the surface. This is in addition to the very rapid changes in conductivity due to the photo generated hole-electron pairs. Consequently the decay of photoconduction was strongly dependent on the ambient gas conditions, being slow in vacuum or an inert gas atmosphere (such as nitrogen) and fast in air. Some important works on photoconductivity of ZnO materials are discussed in this section.

2.1.1 Photocatalysts

The capability to use the solar energy to reduce the organic contaminants makes photocatalysis one of the budding technologies for resolving environment related problems. The TiO_2 photo catalytic arrangement to degrade the pollutants was the first of its kind. Since then several metal sulfides and oxides including ZnO have been recognized as photocatalysts for photo degradation of contaminants. The practical application of these photo catalysts in eradicating environmental pollution has been restrained because of low conversion efficiency of the solar energy and lesser quantum yield. As a result, this area has generated enormous curiosity to be investigated to develop innovative photocatalysts with more versatility and enhanced properties.

Heterogeneously dispersed semi-conductors deliver a proper surrounding to stimulate the chemical reactivity of a large number of adsorbates. They also provide means to start light induced redox reactivity in feebly linked molecules. Upon photo excitation of a few semiconductors non-homogeneously suspended in either fluid or non-aqueous arrangements or in vaporous mixtures, synchronous oxidation and decrease in responses happen. This change regularly achieves either a specific oxidation or a whole oxidative debasement of a natural substrate present. The oxidizing agent in these cases is presumed to be molecular oxygen. However, there is still uncertainly about the mode by which it has been involved in the reactions. The reaction sequence is initiated by that wavelength of the incident light that is absorbed by the semiconductor and not that is absorbed by the substrate. Reactions like these thus involve photosensitization, i.e. photo activation in an indirect way and not the direct development of an excited state of the substrate. Several oxidative conversions can occur per active site of the catalyst without much reduction in the redox catalytic capacity of the semiconductor. This can be attributed to the stability of the photocatalytic materials in those environments.

Fujishima and Honda discovered in the year of 1972 the splitting of water (reduced as well as oxidized at the same time) when a TiO_2 electrode was irradiated and a small electrochemical bias was applied. This insight encouraged far reaching research concentrating on the methods to produce hydrogen (as a combustible fuel) from H_2O by conversion of solar energy. Rapidly it became noticeable that band-gap irradiation of semiconductor particles could induce redox reactions of organic as well as inorganic substrates that are novel in nature **[1]**. Further focussed

investigative enthusiasm for these simultaneous oxidation and reduction reactions has additionally grown inside the most recent decade because of the proposed usage of photo excited semiconductor dispersals in environmental purification and improvement and in illustrating interfacial electron transfer. The likelihood that they might induce synthetically helpful and selective redox changes in explicit organic compounds has started to become increasingly extra striking.

2.2 Metal Organic Frameworks (MOFs)

Metal-Organic Frameworks (MOFs) are chemical compounds that are one, two or three dimensional in structure formed by the co-ordination of metal ions or clusters and rigid organic molecules. Some of the MOF structures can be porous. Proper selection of inorganic metal atoms/ions and organic ligands lead to an array of possibilities in topology and functionalities within MOFs.

Since MOFs have high surface areas and high pore volumes in uniformly sized pores as well as high metal content, they have emerged as interesting materials for various applications in gas storage **[2-4]**, sensors, hydrocarbon adsorption/separation **[5-8]**, drug delivery, catalysis **[9]**, magnetism, CO_2 adsorption **[10-11]**, luminescence, and others. Current extensive review articles on MOFs have dealt with synthesis, characterization, surface modification, and applications.
The structural relationship of some of the MOFs is shown in the figure 1.1.

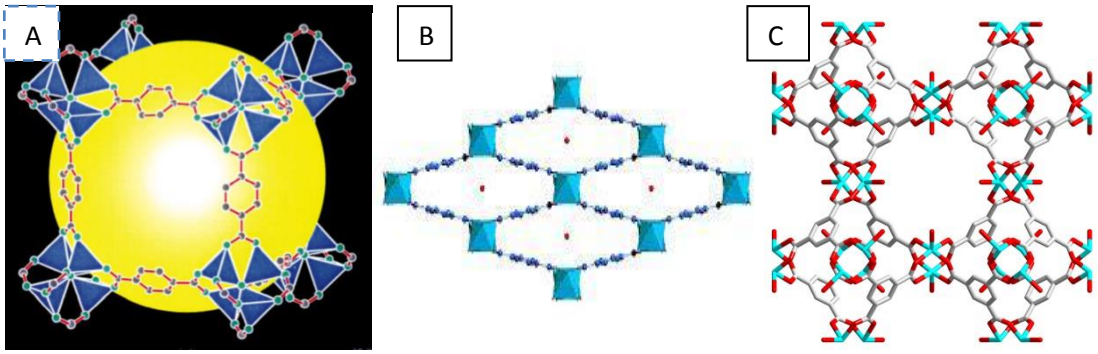

Figure 2.1 Structural relationship of MOFs (A) MOF-5 (B) MIL-53 (Fe) (C) Cu- BTC **[12]**

Up until now, MOFs have been generally prepared via hydrothermal or solvo-thermal synthesis routines by electrical heating in small scales, which take reaction time from several hours to days. Efforts were primarily given to preparing high quality single crystals adequate for structural analysis in dilute liquid phase conditions. Alternative synthesis methods were endeavoured afterwards to shorten the time of synthesis and production of smaller and uniform crystals, such as microwave-assisted, sonochemical, electrochemical, and mechano-chemical methods.

2.2.1 Various applications of MOFs

MOFs have shown tremendous potential to be used in various applications. The major areas are:

1. Hydrogen storage
2. Methane storage
3. Carbon Dioxide storage
4. MOFs as sensors
5. MOFs as magnetic material
6. MOFs as photo-catalysts
7. Gas purification and separation

2.2.2 MOFs as photocatalysts

A very wide range of reactions can be driven by using MOFs. These reactions may include redox reactions, Lewis acid/base catalyzed reactions, asymmetric reactions and photo catalysis. It is easy to separate the MOF catalysts from the reaction mixtures making them possible for reuse. The molecular nature of MOFs offers unparalleled tenability and chemical variety so as to drive a huge number of catalytic reactions. The charge separated excited states of the building blocks formed by photon-excitation can drift across long distances. Hence they can be reaped as redox equals near the MOF-liquid interface via transfer of electrons or by directly activating the substrates that have dispersed into the MOFs structure for photocatalytic reactions. The strong similarities between bulk transition metal oxides and MOFs initiated a few years ago. The first of such instances was examples of the application of metal organic frameworks in photocatalysis. MOF-5 is the best example, where the Zn_4O clusters interconnected by the organic molecules

behave as semiconductor. The organic molecules act as light harvesting antennas. Nevertheless, as the maturity in this field has developed through the years, it is now clear that the electronic properties and chemistry of MOFs may be fundamentally dissimilar from those of classical semiconductors. Subsequently, approaches unalike from those applied in the classical semiconductors to enhance the photo catalytic performance ought to be established for metal organic frameworks **[13]**.

It is because of the optical transitions, photochemical and electrochemical activity that metal organic frameworks have been categorized as semiconductors. However such activities do not necessarily indicate semi conductivity. Inorganic semiconductors are characterized by a delocalized conduction and valence band through which the charge carriers are mobile.

Organic semiconductors are classically characterized by delocalized orbitals via extended conjugated π-bonds, allowing for charge carrier mobility. Delocalization up to a certain degree is necessary in MOFs to display semi-conductive behaviour. Only some MOFs show semi conductivity and is so far of fairly low magnitude. Nevertheless, it has certainly been presented in the literature that holes and electrons are generated in the MOFs upon absorption of light, with oxidative and reductive power respectively, for photocatalysis **[14]**. Photocatalysis consists of an oxidation and a reduction half reaction. When the electrons and holes generated by photo excitation are not mobile, it infers that the reduction and oxidation sites need to be present in close by proximity to the location where the photo excited charges are formed. Unlike in bulk solids, the crystalline nano porous arrangement of MOFs allows a multi modal construction. The spatial vicinity of the photo generated charge carriers though might favour charge recombination competing with the desired redox reactions. On the contrary, the porosity of MOFs facilitates diffusion of products and reactants all through their crystals which can recompense for that. MOFs display exceptional optical tenability unlike the traditional semiconductors such as CdS, TiO_2 and ZnO. In order to deliver the preferred wavelength for absorption, the organic linker molecules can be chosen prior to the synthesis of MOFs. Usually, the optical transitions of curiosity are ligand-to-metal charge transfer (LMCT) in character**.**

Apparently, the orbitals of the metal centres affect the key optical transitions attributed to LMCT. The materials that contain Co-, Cd-, Fe-, and Ni-clusters have been reported to have photo catalytic activity in the visible wavelength region connected to the analogous transitions

originating from the metals. Evidently, explaining the performance of these kinds of materials is conceivable only when the topology of the frameworks is alike. Optical absorption of MOFs can be easily adjusted either by choosing an suitable linker or post-synthetically. As an alternative, the optical response can be engineered by fine-tuning the cluster-forming metal or even by using mixed metal clusters might be an important tool in the future. Manipulations of such kind with absorptive properties can enhance the photocatalytic activity of the frameworks. The organic linkers in the metal organic frameworks may be considered as photon-harvesting units transmitting the energy in the excited states to inorganic Me_xO_y clusters comprising of only a few metal atoms. At such degree of quantization the size of the cluster is too small to impose discrete periodic properties from those found in bulk semiconductors. This kind of tactic typically results in the formation of free charges upon lighting at the suitable wavelength and in moderate to low photocatalytic behaviour. A further intricate method to employ MOFs for photo catalysis is by using them as carriers for photo catalytically active species. This methodology can be utilized for encapsulation of a variety of active sites: from semiconductor nanoparticles to molecular catalysts based on transition metal complexes. All of them have been successfully encapsulated in MOFs. In such cases, the MOF can act either as a simple container or itself take part in the charge transfer process **[13].**

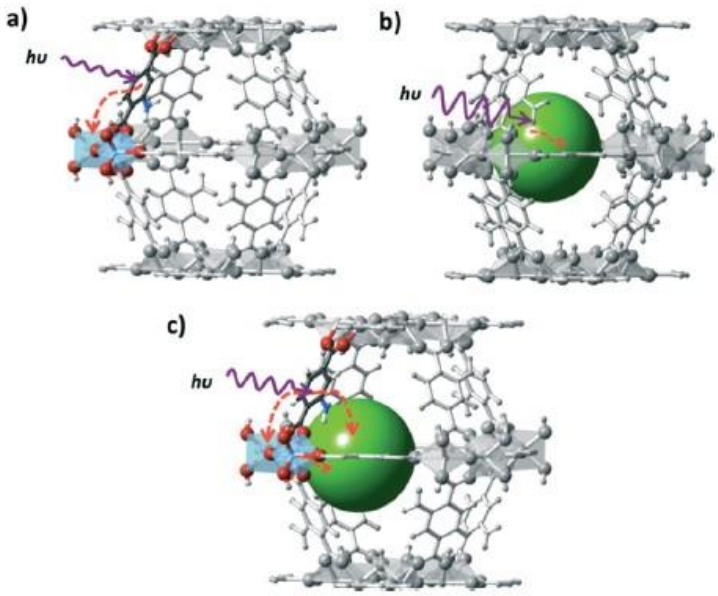

Figure 2.2 Various methods to induce photo catalytic activity in a MOF scaffold:
(a) The organic spacer can be used as an antenna for harvesting light and transferring charge to the metal ions (b) the MOF is used to encapsulate a photo catalyst that absorbs light directly and (c) The transfer of charge occurs between the encapsulated catalyst and MOF scaffold **[13]**

2.2.3 Synthesis of MOFs

MOFs are stereotypically fabricated by associating secondary metal ions with organic linkers to generate varied networks. The metallic ions or the organic linkers can be changed to govern the pore environment of the MOFs, which controls its interactions with adsorbates. This eventually assists its utility for a specific use. Selection of a solvent for these liquid-phase reactions can be based on different aspects such as redox potential, reactivity, stability constant, solubility etc. The solvent plays a significant role in defining the thermodynamics and activation energy for a certain reaction. The slow evaporation technique is a consistent methodology of crystallization which has been requisitioned in the most recent couple of decades to get MOFs **[15-16]**. Even though routine synthesis of MOFs involves solvo-thermal methods, other methods such as microwave-assisted synthesis, electrochemical synthesis, mechano-chemical synthesis and sonochemical synthesis have been used as substitutes for MOF synthesis.

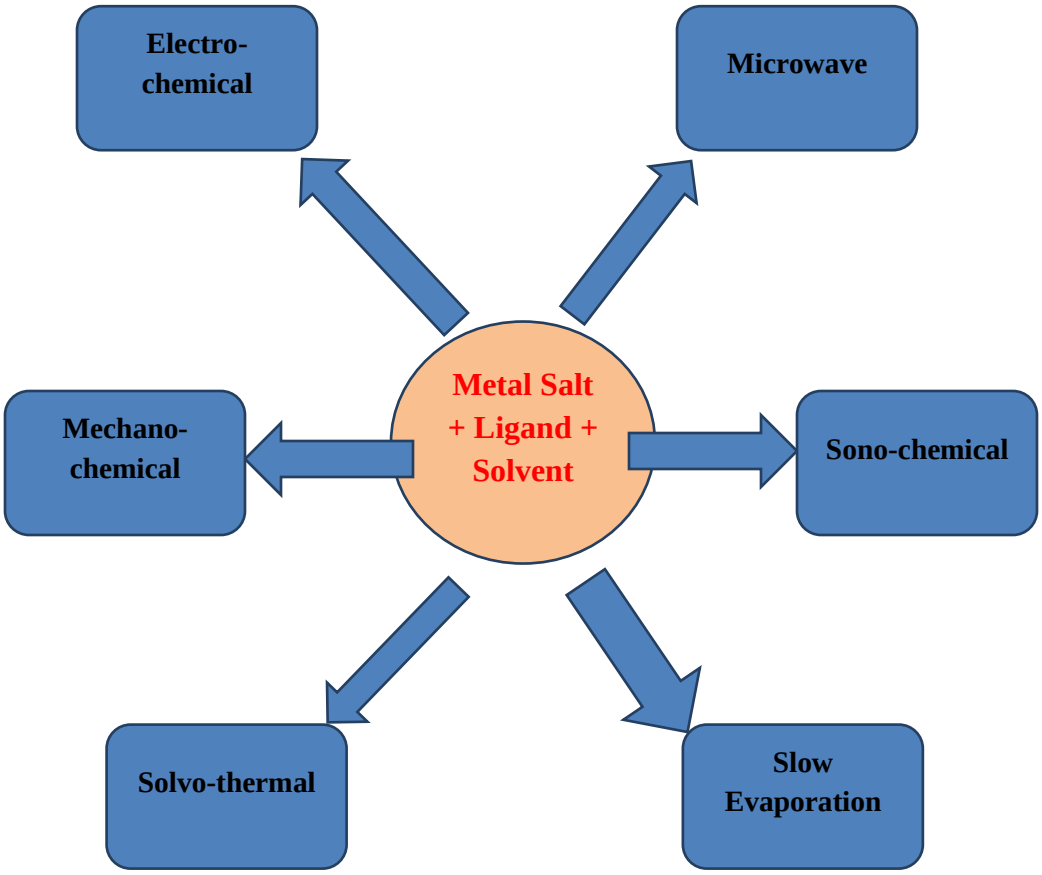

Figure 2.3: Various Methods of synthesis of MOFs

2.3 Transparent Conducting Oxides (TCO)

Initially semi-transparent and electrically conducting CdO film was accounted for as ahead of schedule as in 1907. As the early works on these films were performed out of purely scientific interest, substantial technological advances in such films were observed only after 1940. Enthusiasm for the investigation of transparent semiconductor films has been created primarily by their potential applications in businesses identified with opto-gadgets and photovoltaic device manufacture. Such films have exhibited their utility as transparent electrical radiators for windscreens in the aircraft industry **[17]**. However, during the last decade, these conducting transparent films have been widely used in a variety of other interesting applications such as gas sensors, solar cells, heat reflectors, protective coatings, light transparent electrodes and laser

damage resistant coatings in high power laser technology. Thus scan for other option TCO materials has been a theme of exploration throughout the previous couple of decades. It incorporates some binary materials like SnO_2, ZnO, CdO and ternary materials like $ZnSO_3$, Zn_2SnO_4, $GaInO_3$, $CdSb_2O_6$:Y and so on.

Amid the most recent years, thin ZnO films have been researched widely due to their budding applications as conductive gas sensors, piezoelectric transducers, transparent conductive cathodes, optical waveguides, wave gadgets, acousto-optic media and sun powered cell windows. ZnO, a semiconductor, is currently perceived as a favourable possibility for blue and bright light-emanating diodes or laser diodes. This can be attributed to its wide-band gap of 3.37 eV. ZnO also has a large excitation binding energy (60meV). This large excitation binding energy permits excitonic absorption and recombination even at room temperature making ZnO more appealing. Observations like this show that an excitation linked recombination procedure may be used as an opto-electronic gadget operable at room temperature **[18-19].**

To have an extensive range of applications, abundant ZnO film fabrication techniques have been endeavoured: chemical vapor deposition (CVD), r.f.magnetron sputtering, the sol-gel process and spray pyrolysis. Lately ZnO film production has done by pulsed laser deposition. It can be clearly understood that the thermal excitation of electrons initiated by impurity atoms or defects is responsible for the electrical conductivity of ZnO films at higher temperatures than the ambient temperature. ZnO films deposited by chemical vapour deposition are polycrystalline and for electrical conductivity at ambient temperature band transportation is found to be responsible. This also includes thermionic field emission over the grain boundaries**.**

Significant parameters related to the physical properties of ZnO are tabulated in Table 2.1

Table 2.1 Different parameters of physical properties of ZnO

Density	5.606 g/cm^3
Melting point	1975^{o}C
Thermal conductivity	1-1.2
Stable phase	Wurtzite
Refractive index	2.008-2.029
Energy band gap	3.4 eV, direct
Excitation binding Energy	60 meV
Static dielectric constant	8.656
Electron Hall mobility	200 cm^2/V.s
Lattice parameters at 300 K a_o c_o a_o/c_o	 0.32495 nm 0.52069 nm 1.602

2.3.1 TCO deposition techniques

There are various techniques by which the fabrication can be done. The properties of ZnO films are very much controlled by the growth procedure. The same material fabricated using different methods were found to have dissimilar physical properties. This can be imparted to the fact that the optical and electrical properties intensely depend on the assembly, nature of impurities present and surface morphology. There may be a difference in the physical properties of the films grown by the same particular method. This is due to the difference in deposition parameters. Therefore, the deposition parameters can govern the properties and they can be tailored. It was both important and obligatory to have a thorough study on the different methods used for the fabrication of ZnO films.

2.3.2 Chemical Vapour Deposition (CVD)

CVD is a chemical technique employed to produce good quality and high performance thin films. Low pressure metal-organic chemical vapour deposition method was successfully used for the deposition of ZnO with zinc acetate as precursor solution. Different substrates like In, P, Ga,

As, Si and glass were used and these films were analysed using EDAX and RHEED techniques. Films were poly-crystalline with no preferred orientation. Transparent and conductive ZnO thin films were deposited over Silicon and InP substrates using CVD and characterized using X-ray diffraction (XRD), AFM, optical measurements etc. The significant observation was that the favoured orientation of the ZnO crystallite was along (112) for Silicon and (002) for InP substrates. Studies were done on high quality ZnO grown using MOCVD, over sapphire substrate. High-resolution TEM and XRD analysis were done on these samples. Films were found to be strain free from low temperature photoluminescence studies. Another report on ZnO thin films, prepared using plasma assisted MOCVD on sapphire substrate, was using the results of XRD, photoluminescence and optical transmittance studies. Here also the films were preferentially oriented along (002) plane **[17]**.

2.3.3 Chemical Routes

A fully automatic, Single Ionic Layer Adsorption and Reaction (SILAR) technique was used for the deposition of highly photoconductive and transparent ZnO films. Zinc sulphate and ammonia were the starting solutions. Crystalline films with slight preferential orientation along (002) plane were obtained even at room temperature. Band gap was 3.42 eV for very thin films and it reduced to 3.35 eV for thicker films. A very high photocurrent response (~10^5) was also reported in these films. High quality ZnO thin films were deposited on silica and silicon substrates using 'spin coating technique'. In this method zinc nitrate solution with was used along with glycine. The structure transformed to Wurtzite after the heat treatment at 1000 ºC in air. ZnO buffer layers were deposited over p-$CuInS_2$thin films using Chemical Bath Deposition [CBD] technique to improve the light transmission in the blue region. Here, $ZnSO_4$, ammonia and distilled water were used to prepare the starting solution. The 'as prepared film' contained both Zinc Oxide and Zinc Hydroxide and annealing at higher temperature converted $Zn(OH)_2$to ZnO. Another technique employed was SILAR and experiment was performed at 97 ºC. In this case, ZnO films displayed zincite structure having an average optical transmittance of 80-90%. The efficiency of the cell fabricated using this film was nearly 4%. 'Spin coating technique' was used by *Shimono et al* for the deposition of transparent and conductive ZnO thin films. $Zn(CH_3COO)_2$ mixed with ethanol and diethanolamine was used for the undoped film and $Al(NO_3)_3$ and $Ni(NO_3)_2$ for doping with aluminium and nickel, along with zinc acetate. The

deposited films were amorphous in nature, but after annealing at 500°C it had a wurtzite structure. Sharp absorption edge was obtained at 380 nm. The band gap increased slightly after annealing in hydrogen atmosphere. The prepared films were highly resistive, but the resistivity lowered after post heat treatment in hydrogen **[17]**.

2.3.4 Pulsed Laser Deposition (PLD)

Pulsed Laser Deposition (PLD) technique was a very refined technique for the deposition of ZnO films. In a report, Myoung et al described the effect of film thickness on the properties of laser deposited ZnO thin films. It was seen that crystallinity was improving with the increase in film thickness. Another interesting observation was the decrease in carrier concentration with increase in the film thickness. PL studies revealed two emissions; one in UV region and the other in visible region. Ianno et al. investigated the effect of substrate temperature and laser wavelength on the properties of PLD films. Films were characterized using XRD and optical emission spectroscopy. It was seen that, as the laser wavelength increased to 1064 nm, the films became dull gray in colour. High quality film was obtained at 532 nm radiation. As the laser fluency increased, quality of the film became better. Moreover, the increase in the substrate temperature also, enhanced the film quality. Millon et al reported the deposition of ZnO films on different substrates using femto second pulsed laser. Films were crystalline, smooth, and dense with hexagonal texture. Channelling and rocking curve experiments performed on these films revealed that the film was not as good as that obtained with nanosecond pulses **[17]**.

2.3.5 Molecular Beam Epitaxy (MBE)

Plasma assisted Molecular Beam Epitaxy (P-MBE) technique has been used to develop ZnO thin films on Al_2O_3substrate, under various Zn/O ratios. Highest quality ZnO was obtained when stoichiometric flux conditions were applied. It was seen that, the growth rate increased when Zn flux increased. It was also observed that with the increase in growth temperature, Zinc flux should be increased to grow the desired stoichiometric films. Surface analysis revealed the presence of hexagonal shaped 2D islands. XRD and PL studies were also used on these samples.

An interesting report was on MBE grown ZnO films over lattice matched $ScAlMgO_4$ substrate. To avoid, even the very small (0.09%) lattice mismatch, a buffer layer of ZnO annealed at high

temperature was used. On the surface of annealed ZnO buffer layer, ZnO films were fabricated with varied laser replication conditions. Crystallinity of the material was analyzed using high resolution XRD. Flat surface was obtained with low laser repetition, while terrace and step structures were observed at higher repetition. Low temperature PL measurements were also done to identify excitonic emissions **[17]**.

2.3.6 Sputtering

Effects of r-f sputtering power, rate of deposition and temperature of the substrate, the pressure of chamber on the properties of zinc oxide thin films were the major areas to be studied. It was seen that perpendicularly oriented ZnO films were obtained with lower rate of deposition and at lower temperature of the substrate. Sputtering parameters were found to strongly influence the grain size. Optical properties of ZnO films, grown using r.f sputtering technique on sapphire substrate, were stated by Valentini et al. The films were rather homogeneous and high optical transmittance [~ 85 % in the visible region] with sharp optical absorption edge at 380 nm. Refractive index was also calculated from reflectance spectra in this paper and values were in the range of 1.9 - 2.1. In another paper, structural analysis of r.f. sputtered ZnO films were reported. Studies using XRD and SEM were done on these films having different thickness and prepared at different substrate temperature. Grain size increased with increase in the thickness of film and also with the increasing substrate temperature **[17]**.

2.3.7 Spray Pyrolysis

Spray pyrolysis technique was used to prepare ZnO thin films with different precursors such as $ZnCl_2$ and Zn acetate. By suitably adjusting the deposition parameters, a resistivity of 10-3ohm cm could be achieved. It was seen that, the presence of Cl in the films reduced the resistivity. The photoconductivity of the films was ascribed to desorption of oxygen from the film. The properties of ZnO films grown on various substrates by ultrasonic spray pyrolysis method was reported by Wu et al. Single-phase homogeneous uniform films having band gap of 3.27 eV, were obtained by this technique. Particle size was around 5 μm.

This technique was used to investigate the effect of substrate temperature on the properties of ZnO thin films grown on alumina substrate. Concentration of starting solution was also varied.

The fastest deposition rate occurred between 400 and 450ºC. In this temperature range, the films were uniform, dense and oriented along (002) direction. Goyal et al discussed the effects of concentration of precursors on the various properties of ZnO films. Growth rate and crystalline quality increased with increase in the concentration. Texture coefficient of (002) plane also increased with the increase in molarity of solution **[17]**.

2.4 ZnO based Transparent Conducting Oxides (TCO)

Thin film photovoltaic advances are being considered as a method for significantly lessening the expense of photovoltaic frameworks. The basis for this is that thin film cells are required to be less expensive to fabricate inferable from their lessened material, taking care of capital expenses. Semiconductor thin films simultaneously displaying high electrical conductivity and optical transparency are of major technical significance, for instance in solar cells, flat panel displays, and electrical devices. The requisite amalgamation of properties can be recognized by degenerate doping of wide band gap oxide semiconductors such as ZnO, In_2O_3, TiO_2 or SnO_2.

Of all these, ZnO displays high optical transmittance and this has projected it as the most widely used Transparent Conductive Oxide (TCO) in developing many optoelectronic devices. Because of the high crystallinity and trimness of the subsequent thin films, fabulous electrical conductivities can be attained to under the advanced preparative conditions.

In recent years, Zinc Oxide thin films have fascinated much consideration due to their prospective application in optical waveguides, solar cells, surface acoustic devices, gas sensors, piezoelectric transducers etc. The ultraviolet radiation from the excited ZnO thin film is noticed and this makes it conceivable to manufacture ultraviolet laser devices. Furthermore, numerous light emitting devices (like blue light, green light and purple light) can be manufactured by ZnO films.

The optical properties of ZnO thin film are much affected by both the growth procedures and also the film assembly. Particularly, the (002) c-axis oriented ZnO film displays finest optical behaviour. ZnO has gained ample attention because of the numerous benefits over the other oxide thin films such as In_2O_3, SnO_2 or $CdSnO_4$. These benefits comprise of good electrical, optical behaviours, non-toxicity, stability in hydrogen plasma atmosphere and being cheaper. A

standout amongst the most critical qualities of ZnO is that it has vast excitation energy (~60 meV) **[18].**

2.5 The Sol-Gel Process

The Sol-gel process, commonly identified as chemical solution deposition, has an extensive array of applications in ceramics and materials science. This process permits formation a solid substance by making use of a solution or a gel as a midway step, and at temperatures lesser than that is conceivable by old preparation techniques. This facilitates the powder-less processing of glasses, ceramics, thin films or fibres straight from the solution. The manufacturing of solid materials via soft chemistry usually includes sol–gel and wet chemistry reactions based on the transformation of molecular precursors into a network of oxides by hydrolysis and condensation reactions **[19-20]**.

The procedure comprises of the steps as stated below:

- A stable solution is made by using precursors
- The solution is transformed into gel by addition of appropriate reagent
- The gel is allowed to age and mature into a compact mass
- Deposition of the prepared gel on the substrate by the selected method
- The gel is dried so as to remove any residual liquid phases
- The compact mass formed is annealed at a high temperature in the furnace

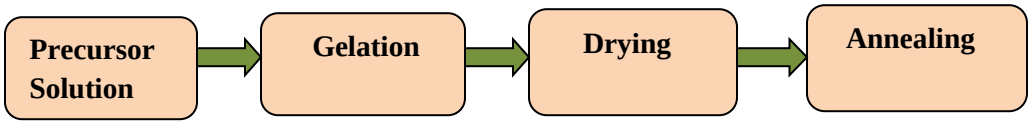

Figure 2.4 Schematic illustration of the Sol-gel process

Sol-gel procedure is a cheap, continuous and basic technique giving higher yield. The upsides of this strategy incorporate getting high virtue materials, process flexibility, simplicity of integrating uncommon materials and saving energy by utilizing low operation temperatures.

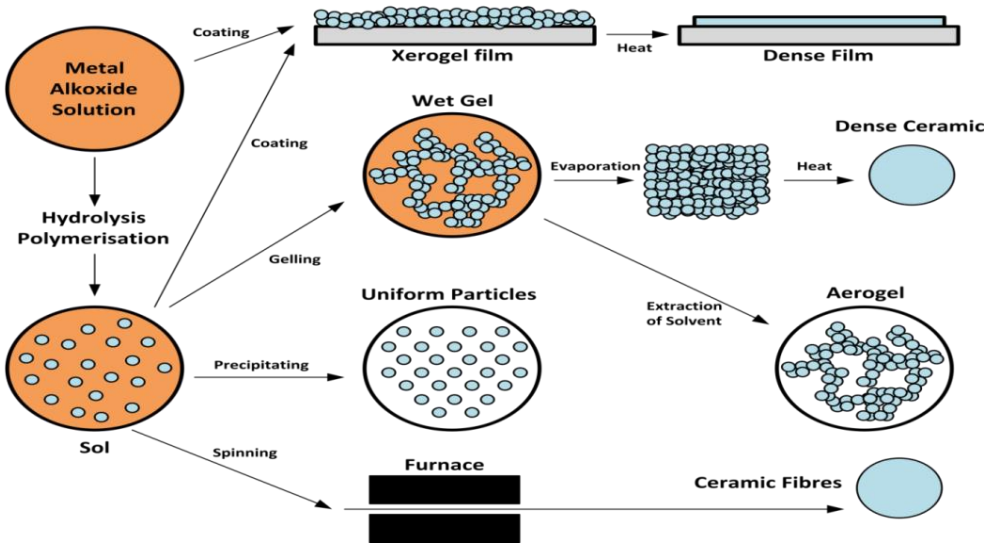

Figure 2.5 Various Sol-gel techniques and their products **[20]**

ZnO thin film fabrication includes many parameters: (1) the type and concentration of precursor (2) nature of solvent as well as the acidity of the medium, (3) the aging time of the gel, (5) the coating technique used and its speed, (6) the nature of the substrate on which the deposition is done, and (7) the pre- and post-heat treatment of the mass formed at high temperature in the furnace. The literature survey shows that these factors play a vital role in the development texture of zinc oxide films **[20]**.

2.6 Effect of annealing temperature on ZnO films

Sengupta et. al concluded that almost all the fabricated ZnO thin films regardless of the annealing temperature had desired c-axis orientation. The most stable form being thehexagonal wurtzite structure. Also the degree of preferred orientation, crystallinity and average grain size of the films increased with the increase in annealing temperature. It was also revealed from the diffractograms that the preferred orientation along (002) was mutual in all the films. It was also seen that the intensity of (002) peak progressively increased with the increasing annealing temperature. Good percentage of transparency was also observed for the annealed ZnO films in wavelength region of 400-800 nm. Sharp edges of absorption were exhibited in the transmittance spectra at around 380 nm wavelength. They found out that there was a decrease in transmittance

with the increase in annealing temperature. This could be described by the increased surface roughness of the deposited films. The whole of the samples exhibited decent homogeneity and there were no cracks to be noted. From the AFM images, it was witnessed that the grain sizes become bigger with the rise in annealing temperature **[21]**.

2.7 Doped ZnO

Doping ZnO with impurities makes it a probable candidate for being used as transparent conducting oxides (TCOs) so that it can have budding applications as a electrode. ZnO is available in plenty, is non-hazardous, and inexpensive. To add to its value, impurity-doped ZnO can be supposed to have electrical and optical properties analogous to the costly indium tin oxide (ITO).

2.7.1 Aluminium Doped Zn-TCO

A very simple and easy non-alkoxide sol-gel method for deposition of Al-doped ZnO transparent conducting thin films on the glass had been reported by *Gil Mo Nam et al*. This method uses 2-methoxyethanol and mono-ethanolamine (MEA) as solvents and aluminium nitrate as the dopant precursor. The starting material used for making ZnO was Zinc acetate di-hydrate ($Zn(CH_3COO)_2 \cdot 2H_2O$). Equimolar amount of 2-methoxyethanol and mono-ethanolamine (MEA) were used as solvents.0.75 molar concentration of Zinc acetate di-hydrate was made by dissolving the proper quantity of it in the solvent. The Al percentage is defined by 100*{(Al/(Al+Zn)}. The resulted is the formation of a clear solution which was aged at room temperature for 2 days. Then the Al-doped ZnO thin film was spin-coated onto a SiO_2-deposited soda lime glass substrate having a thickness of 1.1 mm. The spin-coating was carried out at 3000 rpm spinning rate, for 30 sec and at ambient temperature. The coated film was preheated in air for 15 minutes and at 350℃ after each cycle. The whole process of spin coating and preheating was continued for 6 cycles to get the required thickness. After the total number of cycles was over, the first post-heat treatment was done in air at 530℃. Then the second post heat treatment was carried out at 500℃, in a reducing atmosphere of 5% H_2 - 95% N_2. After both the post heat treatments, it was observed that all the films displayed hexagonal-phase crystallization. All the trials (0% to 5.0%-Al-doped ZnO) showed a c-axis favoured orientation. Also, the peak width widened with the rise in Aluminium concentration, which is suggestive of the fact that the crystal size of the ZnO:Al thin film decreases with the increase inAl concentration. Many pores were

seen in the un-doped ZnO thin film. The grain size of the film containing aluminium (0.25%) was considerably smaller as compared to the undoped ZnO thin film. The grain size was found to decrease with the increase in Aluminium concentration. This could be easily anticipated from the widening of the peak in the XRD pattern **[22]**.

2.7.2 Fluorine doped Zn-TCO

A very simple and easy sol-gel method had been proposed by *Gil Mo Nam et. al*for the deposition of Fluorine-doped Zn-TCO thin films on glass. The solvents used were 2-methoxy-ethanol and mono-ethanolamine. Zinc acetate was used as the starting material for Zinc Oxide and Aluminium Fluoride was used as the source of Fluorine. An equimolar amount of 2-methoxy-ethanol and mono-ethanol-amine (MEA) was used as the solvent. 0.75M Zinc dihydrate solution was prepared by dissolving it in the solvents. Using NH_4F as the precursor the Fluorine concentration was varied upto atomic percentage of 10%. This resulted in a clear solution which was aged for 2 days at ambient temperature. Then spin coating technique was used for fabricating F-doped ZnO thin film onto a Silica deposited soda lime glass substrate with a thickness of 1.1 mm. The spin-coating was carried out at 3000 rpm spinning rate, for 30 sec and at ambient temperature. The coated film was preheated in air for 15 minutes and at 350℃ after each cycle. The whole process of spin coating and preheating was continued for 6 cycles to get the required thickness. After the total number of cycles was over, the first post-heat treatment was done in air at 530℃. Then the second post heat treatment was carried out at 500℃, in a reducing atmosphere of 5% H_2 - 95% N_2. The structural, electrical, and optical properties of the spin-coated ZnO-F thin film on glass were analysed at various Fluorine dopant concentration. Those properties were also examined at various post heat treatment temperature values. The variations in carrier density, structure, transmittance and mobility were studied as a function of Fluorine concentration **[23]**.

2.8 Synthesis of MOF-5

MOF-5 (Zn_4O(1,4-benzenedicarboxylate)$_3$) is the one of the most investigated metal-organic framework. It has been widely studied because of its high surface area and the low cost raw materials. There are various synthetic techniques that have been established with the objective of

attaining higher surface area as well as larger pore volume. Usually, mass transfer techniques, solvo-thermal techniques or atmospheric pressure method of synthesis can are applied to synthesizeMOF-5.Because of the requirement to reduce the time of synthesis and to increase the energy efficiency, new techniques with the use of ultrasounds and microwave irradiation were established **[24-25].**

Gabriela Blăniţă et al. [] proposed the procedure for making MOF-5 by microwave synthesis. A particular temperature sensor of the microwave is used to control the temperature of the reaction. This controller has high sensitivity and works over a large range of temperature. The zone for treatment is a microwave cavity that has a coaxial geometry. It was estimated that the cavity would present maximum volume for the mono modal distribution at a frequency of 2.45 GHz. This kind of distribution of microwave power density permits quick treatment with maximum energy transfer. The filling factor of the microwave pulse was set at 40% for MOF-5(μw) synthesis; the temperature was set at 80°C. The time duration of the process was 210 seconds. Upon investigation, the XRD pattern of microwave synthesized MOF-5exhibited broader Bragg reflections than solvothermal synthesized MOF-5pattern. This indicates the presence of smaller crystal structure. A peak in the XRD pattern appears at $2\theta = 8.8°$ for both MOF- 5(μw) and MOF-5(s). This is linked with water effect on MOF-5 structure **[25]**.

2.9 Photo catalytic degradation of Ammonia

The occurrence of ammonia pollution in water is a key menace to the environment as well as human health. Ammonia is one of the vital nitrogen-containing pollutants which reduces decontamination efficacy of chlorine, reduces the dissolved oxygen and displays severe harmfulness to marine life in wastewater discharges. The leading sources of ammonia pollution in wastewaters include dyes, fertilizers, herbicides, metal plating, pesticides, chemicals, industrial solvents, petrochemicals and industrials. Numerous techniques have been suggested for removal of ammonia from wastewater. These techniques include stripping, biological process, breakpoint chlorination, electrochemical process, ion exchange, and photocatalysis. Degradation of ammonia by the photocatalytic method is interesting due to its preferential physiognomies like simple operation, negligible generation of secondary waste, remote control,

high-efficiency and low cost. Different structures of nano-TiO_2 have been used for photocatalytic degradation of chemical contaminants. In the interim, many researchers have reported the photodegradation of ammonia. The photocatalytic oxidation is initiated by bright (UV) light illumination. In photocatalytic responses, the produced positive hole (h+) and electron (e−) have a noteworthy part. Also, the hydroxyl created from the disintegration of water encourages oxidation of ammonia into N_2 **[26-28]**.

CHAPTER- 3

EXPERIMENTAL WORK

This section explains all the experimental procedures that were carried out during this research work.

3.1 Overview

(a) Synthesis of MOF-5 and MIL-53(Fe)

(b) Characterization of MOF-5 and MIL-53 (Fe)

(c) Synthesis of MOF-5 using Zinc Oxide

(d) Characterization of MOF-5 using Zinc Oxide

(e) Preparation of ZnO-TCO

(f) Characterization of TCO

(g) Embedding MOF-5 on TCO

(h) Degradation of Ammonium ion (Kinetics)

3.2 Materials/Chemicals used:

All chemicals utilized in this work for various synthesis methodologies were used as supplied without further purification.

3.2 1 Synthesizing MOF-5

(a) Zinc Nitrate Hexa-Hydrate (b) Dimethyl Formamide (DMF) (c) Terephthalic acid (BDC) (d) Water

3.2.2 Synthesizing MOF-5 from Zinc Oxide

(a) Zinc Oxide (b) Terephthalic acid (BDC) (c) DMF

3.2.3For making Zinc Oxide films (TCO)

(a) Zinc Acetate (b) Ethylene Glycol (c) Glycerol (d) Tri-ethylamine (e) Glass support

(f) Methanol

3.3 Equipment used

1. *Hot Air Oven*
2. *Muffle Furnace*
3. *Tubular Furnace*
4. *Microwave Reactor*
5. *Spin Coater*
6. *Mercury Vapor Lamp Box*

3.4 Experimental Procedure

3.4.1 Microwave Synthesis of MOF-5

A solution of 0.9g of Zinc Nitrate hexa-hydrate in 50 ml DMF was made. This solution was then mixed with a solution of 0.169g terephthalic acid (98%) in 48 ml DMF and 2ml water. The resulting solution mixture was put into a glass vial. The pulse of the microwave was fixed at 40%. The reaction temperature was then set at 80^{o}C and the duration of the whole process was 210 seconds. Then microwave irradiation was started. The product mixture was permitted to cool to the ambient temperature after the process was completed. The solvent was drained off and the residual solid was washed with anhydrous DMF six times. Each time the solid was left to get soaked in DMF for nearly 12 hours. The product formed was then filtered and preserved for characterization.

Yield- 47-50%

The process was repeated many times in various batches to accumulate large amount product for further characterization and analysis.

3.4.2. Microwave synthesis of ZnO-MOF-5

0.163g of ZnO and .083 g of BDC is mixed in 50ml DMF and kept for stirring for sufficient period of time. The solution was then put into 30ml glass vials and put into the microwave reactor at 120^{o}C for 1 hour. After the product was formed it was then brought down to the room temperature and the liquid was siphoned out. The crystals were washed with DMF and preserved for characterization.

The process was repeated many times in various batches to accumulate large amount product for further characterization and analysis.

3.4.3 Microwave synthesis of MIL-53 (Fe)

Fe-BDC or MIL-53 was synthesized as following. The reaction was carried out in glass vial where a stoichiometric mixture of $FeCl_3.6H_2O$, DMF and 1, 4-benzene dicarboxylic acid was placed in microwave reactor for different parameters.

3.4.4 Making the TCO by sol-gel spin coating technique

The solution mixture was made using Zinc Acetate di-hydrate, ethylene glycol, methanol, triethylamine and glycerol.10g Zinc Acetate Di-Hydrate was taken in a round bottomed flask to which 3 ml of ethylene glycol was added. The flask was kept at a temperature of 150^{o}C for nearly 20-25 minutes to obtain a uniform and transparent solution. Water vapour evolved from the mixture during the heating which is equivalent to the water of hydration in $Zn(CH_3COO)_2.2H_2O$. Upon being cooled to the room temperature, the content of the flask solidified to a transparent brittle solid. Alcohols such as methanol, ethanol, n-propanol etc. could be used to dissolve the solid formed. 0.5 ml of glycerol was added to enhance the solubility and film formation property of the solution. Triethylamine (2ml) was also added to assist the hydrolysis of Zinc acetate.

The glass slides were first ultra-sonicated with distilled water for 10 minutes. Then they were ultra-sonicated with acetone for 10 minutes. After ultra-sonication they were kept in the hot air oven for some time. This part is the cleaning of the glass slides on which the coating is to be done.

ZnO thin films were fabricated by the spin coating technique. 1ml of the precursor solution was dropped on the cleaned glass slides and spun at 3000 rpm for 40 seconds. After spin coating, the glass slides were kept at 80^{o}C for 10 minutes for drying. Then the coating cycle was continued until the desired numbered of cycles were completed. These films were then slowly annealed at about 550^{o}C for about 20 minutes to make them polycrystalline.

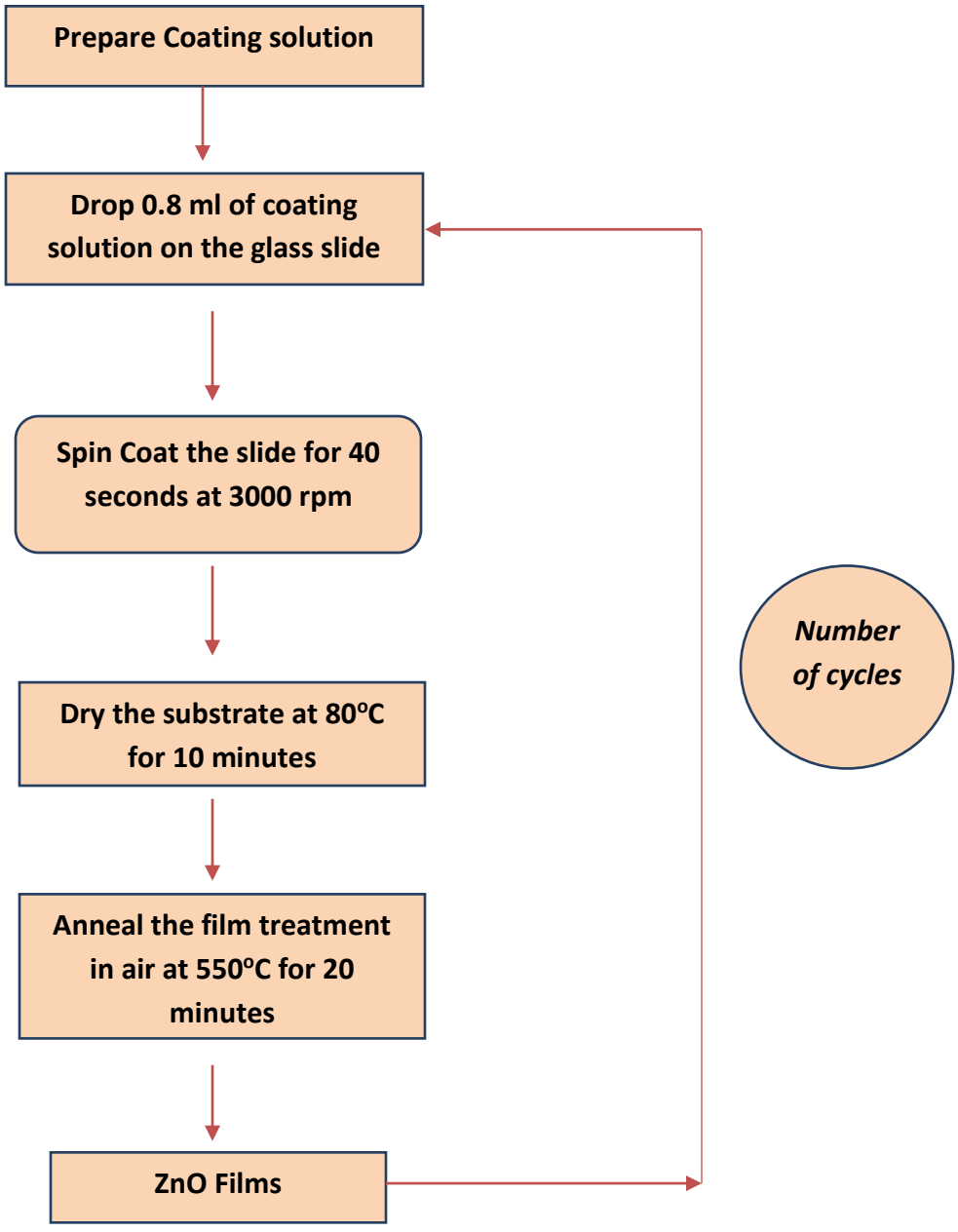

Figure 3.1 Outline for making ZnO TCO

3.4.5 Making the Lead doped ZnO-TCO

Lead percentage – 1%, 2%.

The solution mixture was made using Zinc Acetate di-hydrate, ethylene glycol, methanol, triethylamine and glycerol.10g Zinc Acetate Di-Hydrate was taken in a round bottomed flask to which 3 ml of ethylene glycol was added. The flask was kept at a temperature of 150^{o}C for nearly 20-25 minutes to obtain a clear and transparent solution. Water vapour evolved from the mixture during the heating which is equivalent to the water of hydration in $Zn(CH_3COO)_2.2H_2O$. Upon being cooled to the room temperature, the content of the flask solidified to a transparent brittle solid. Alcohols such as methanol, ethanol, n-propanol etc. could be used to dissolve the solid formed. 0.5 ml of glycerol was added to enhance the solubility and film formation property of the solution. Triethylamine (2ml) was also added to assist the hydrolysis of Zinc acetate.

Lead Nitrate of the required quantity was added by dissolving it in the methanol, triethylamine and glycerol mixture.

Number of cycles- 7, 8 and 9

3.4.6 Making the Aluminium doped ZnO-TCO

Aluminium percentage –1%, 1.5%, 2%, 2.5%, 5%, 10%, 18%, 30%

10g Zinc Acetate Di-Hydrate was taken in a round bottomed flask to which 3 ml of ethylene glycol was added. The flask was kept at a temperature of 150^{o}C for nearly 20-25 minutes to obtain a clear and transparent solution. To this the calculated amount of Aluminium Nitrate dissolved in 20 ml of methanol was added. The resulting solution was used for spin coating.

Number of cycles- 10

3.4.7 Degradation of Ammonium ion (KINETICS)

3.4.7.1 Phenate Method

The Phenate method is most widely used to determine the concentration of Ammonium ion.

Principle: Indophenol, an intense blue compound, is formed by the reaction of ammonia, hypochlorite and phenol in the presence of sodium nitroprusside as catalyst.

Optical density is measured at 640 nm.

- Phenol solution: 11.1 ml of liquefied phenol was mixed with ethanol (95% V/V) to make up to 100 ml.
- Sodium Nitroprusside: 0.5 g Sodium Nitroprusside was dissolved in 100 ml of water. Stored in Amber bottle.
- Oxidizing Solution: 25ml Sodium Hypochlorite made up to 100 ml with water.
- Stock Solution NH_4^+: 38.2 mg NH_4Cl

3.4.7.2 Standard Method (For NO_2^-)

- Buffer colour reagent: 1. 52.5 ml conc HCl
  2. 2.5g Sulfanilamide
  3. 0.25g N,N Napthyl ethylene diamine dihydrochloride
  4. Make upto 100 ml.
  5. 65g sodium acetate is dissolved.
  6. Made upto 250 ml.
- Stock Solution (Nitrite): 1. 0.1493g anhydrous $NaNO_2$ in 100 ml water.
  2. On top add 2ml $CHCl_3$(chloroform)

3.4.7.3 Standard Method (For NO_3^-)

- Stock Solution (Nitrate): 0.38g KNO_3 in 100ml water.
- Reducing Solution: 1g Zinc dust and 50g NaCl in 100 ml water.
- Dilute HCl: HCl:H_2O = 1:4 (Total 100 ml)

Procedure

0.038g of Ammonium chloride was dissolved in 100ml water. 20 ml of this was taken in each of the 3 vials for investigating the kinetics. ZnO, MOF-5 and MIL-53 (Fe) were used as photo catalysts.

Quantity of ZnO – 30mg

Quantity of MOF-5 – 10mg

Quantity of MIL-53 (Fe) - 10 mg

Before the addition of catalysts 1.5 ml of the samples from each vial was siphoned out. After the addition of catalysts the samples were continuously stirred and were kept in the UV lamp chamber. 1.5 ml was siphoned out at regular intervals, then centrifuged and the catalyst free solution was preserved for ammonium ion concentration estimation using the Phenate method.

The percentage degradation and rate constants were calculated.

CHAPTER 4

RESULTS AND DISCUSSION

Various experimental findings are detailed in this section.

4.1 PXRD patterns of Zn-BDC (or, MOF-5)

The powder XRD patterns of Zn-BDC are shown in **Figure 4.1**. The typical peaks formed were characteristics of Zn-BDC and was seen within the two theta (2θ) range of 5° to 20°.The material was found to be crystalline and the unit cell data was calculated by processing PXRD patterns. It was noted that the method of synthesis and solvent used affects the formation of crystals, the size of crystal, its unit cell properties and finally the surface area.

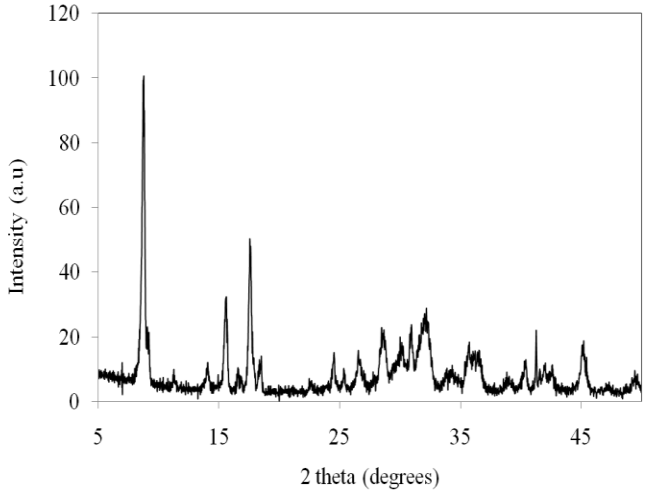

Unit Cell Parameters	
a [Å]	10.075
b[Å]	10.075
c[Å]	6.965
α[°]	90
β[°]	90
γ[°]	90
Volume [Å^3]	706.98
Crystal System	Tetragonal
Space group	P 42/m m c

Figure 4.1 PXRD pattern of MOF-5 along with Unit cell parameters

4.2 TGA pattern of MOF-5

The thermal stability of MOF-5 has been studied by Thermo-Gravimetric Analysis (TGA) and the pattern is as shown below.

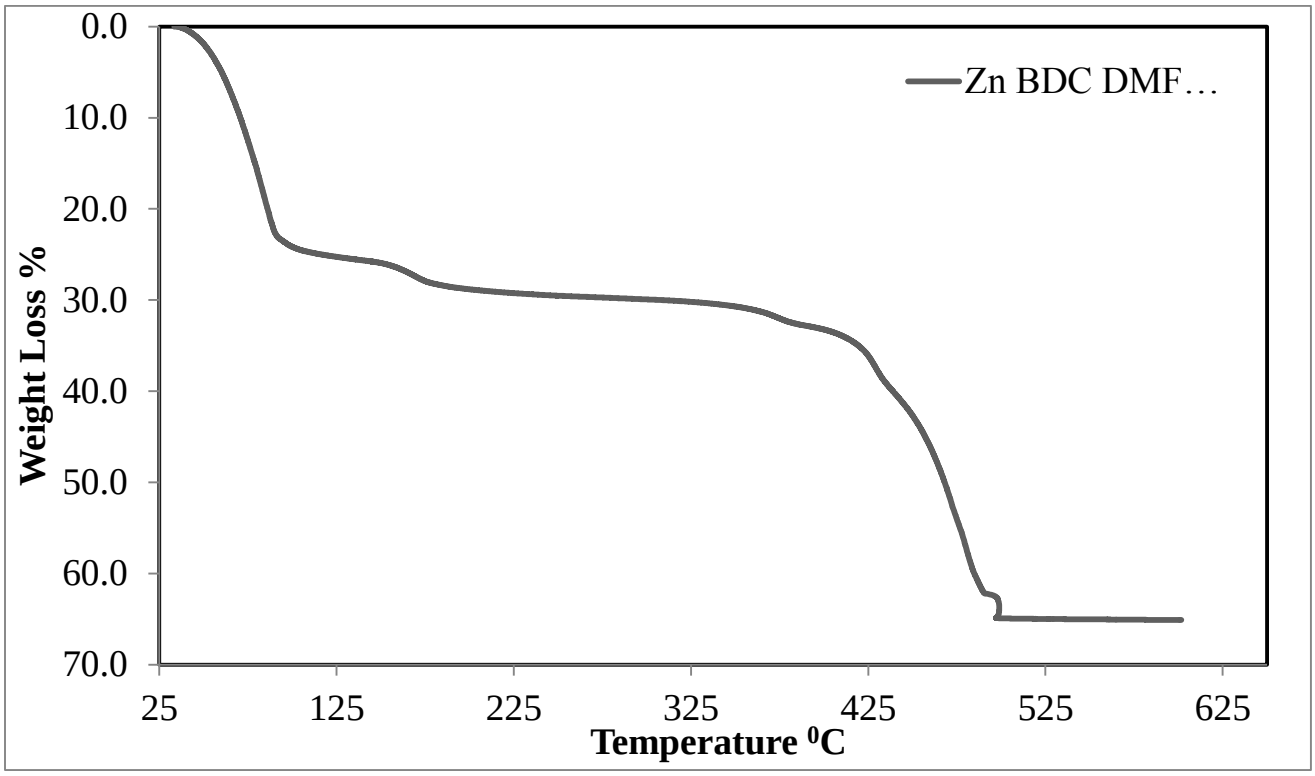

Figure 4.2 TGA plot of MOF-5

The first weight loss that occurred between 50 and 120°C can be attributed to a loss of moisture or water, while the second weight loss step that occurred between 130 and 180°C corresponds to the loss of DMF molecules from the interior of the porous framework. The major weight loss starting at nearly 400°C corresponds to the decomposition of MOF-5 framework.

4.3 BET Surface Area Analysis of MOF-5

One of exquisite feature of any metal organic framework is that it possesses very high specific surface area and BET isotherm studies were performed in the relative pressure range of 0.05 to 0.35, giving total surface area of DMF treated Zn-BDC sample as 856.0 m^2 g^{-1}.

4.4 Surface Morphology of MOF-5

MOF-5 is known to form crystals in cubic lattice system and the morphology of Zn-BDC sample synthesized in this work is shown in the **Figure 4.2**. The SEM image established the fact that, after DMF treatment, Zn-BDC samples were devoid of any unreacted H_2BDC as impurities and the crystals formed were cubic in nature.

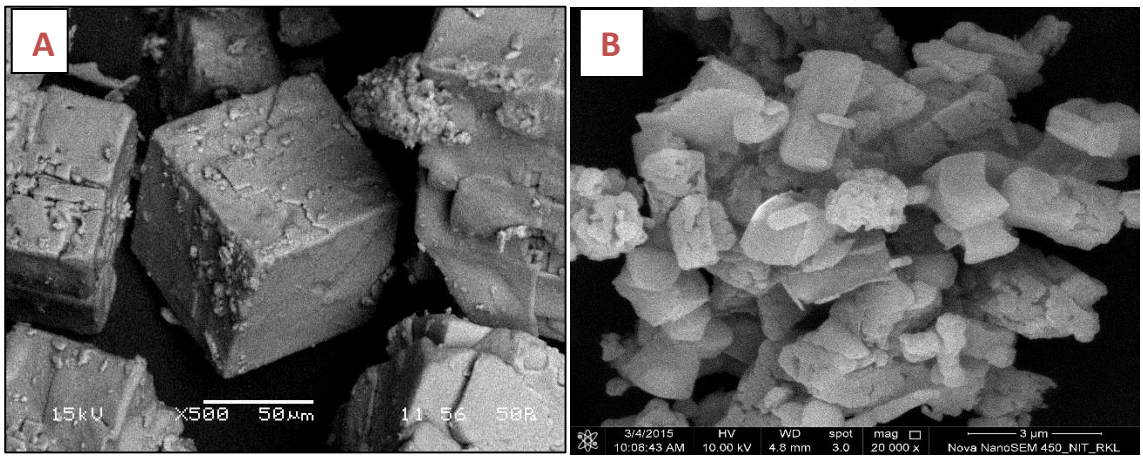

Figure 4.3 SEM image Zn-BDC or MOF-5 (DMF treated) A. Solvothermal B. Microwave

4.5 PXRD patterns of Fe-BDC (or, MIL-53 (Fe))

The powder XRD patterns of Fe-BDC are shown in **Figure 4.3**. The typical peaks (within the two theta (2θ) range of 9º to 25º) were characteristic features of Fe-BDC, confirming the product formation in pure phase. The unit cell data was calculated after processing the PXRD pattern.

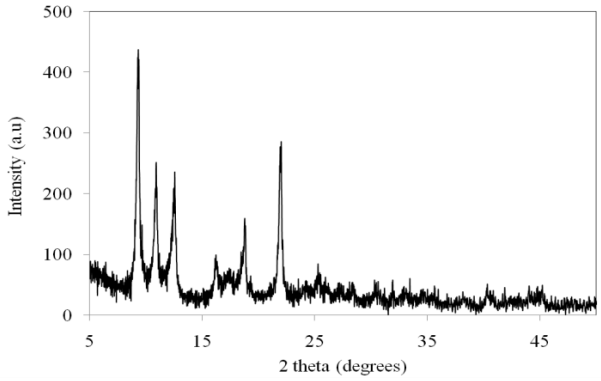

Unit Cell Parameters	
a [Å]	10.95
b[Å]	9.272
c[Å]	8.11
α[°]	90
β[°]	90
γ[°]	90
Volume [Å^3]	823.524
Crystal System	Orthorhombic
Space group	P 21 2 2

Figure 4.4 PXRD pattern of Fe-BDC along with unit cell parameters

4.6 Thermo-gravimetric Analysis of Fe-BDC

The TGA profile of Fe-BDC sample is shown in **Figure 4.4**.

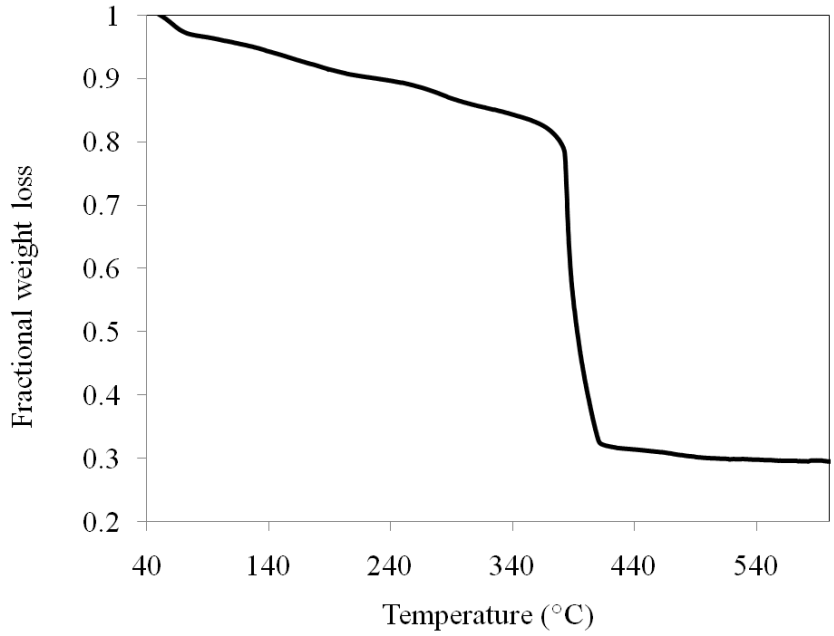

Figure 4.5 TGA profile of Fe-BDC (after DMF treatment)

This typical TGA profile shows three distinct weight loss steps. Initially, within the temperature range of 25-150ºC, the weight loss was purely due to removal of moisture and trapped DMF. The second step, from 160ºC to 360ºC was a fairly horizontal plateau region, where the weight loss

remained fairly constant and it was in this range of temperature, Fe-BDC was found thermally stable. Finally, beyond 360^{o}C, the MOF structure collapsed, owing to the instability of the H_2BDC organic linker.

4.7 BET Surface Area Analysis of Fe-BDC

The porous nature of Fe-BDC was established by carrying out BET surface area analysis within the relative pressure range of 0.05 to 0.35 in liquid N_2 temperature. The surface area of the synthesized product was found to be *ca*. 120 m^2 g^{-1}.

4.8 Surface Morphology of Fe-BDC

Fe-BDC or MIL - 53(Fe) is known to form crystals in orthorhombic lattice arrangement and the crystals of Fe-BDC synthesized in this work is shown using SEM image below. Clearly, from **Figure 4.5**, it might be concluded that the absence of any significant amount of cylindrical shaped H_2BDC from the product was due to DMF treatment.

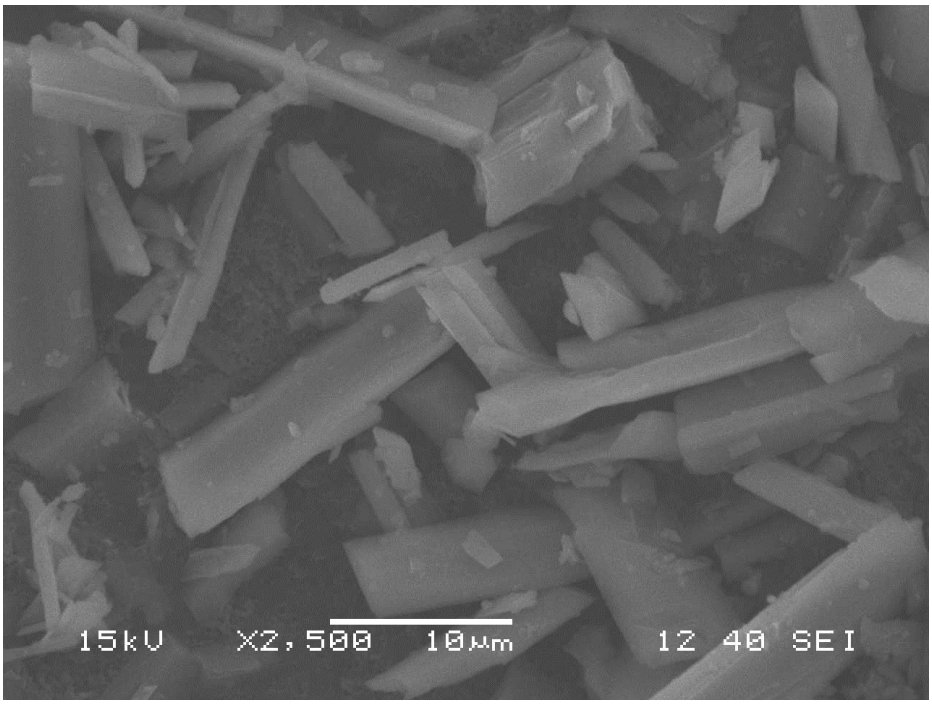

Figure 4.6 SEM image of Fe-BDC or MIL-53 (Fe)

4.9 XRD patterns of Zn-TCO

The XRD pattern of different cycles of Zn-TCO is shown in the **Figure 4.6**.

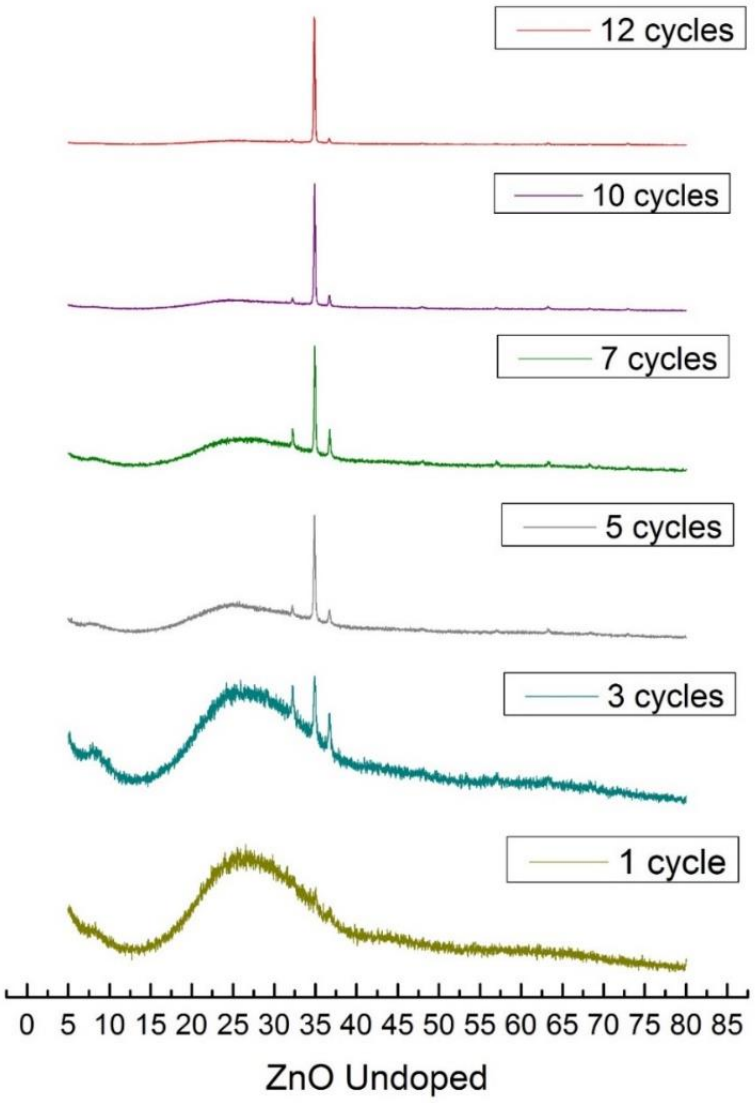

Figure 4.7 XRD patterns of various cycles of Zn-TCO

Polycrystalline nature of the ZnO film was clearly shown by the XRD pattern. The films showed a preferred *c*-axis growth which was oriented normal to the glass substrate. The (002) peak in the XRD pattern was found at 2Θ equal to 38 which was in agreement with the literature. The (002)

peak intensity increased with the increasing temperature of annealing. But the full width at half-maximum FWHM of the 002 peaks didn't change much with increasing temperature of annealing. Therefore, the overall c-axis growth of the films was considered not being disturbed by the piling up of ZnO film or multiple coating. The c-axis orientation of ZnO films was also stated for other techniques of fabrication on glass substrates. Consequently, the c-axis orientation may be a common phenomenon occurring in the ZnO film deposition using organo-zinc compounds.

4.10 Surface Morphology of Zinc Oxide (Undoped) based TCO

The FESEM images (**Figure 4.7**) clearly shows various coating cycles. The observation inferred is that the particle size of thin film coat is within several nanometres.

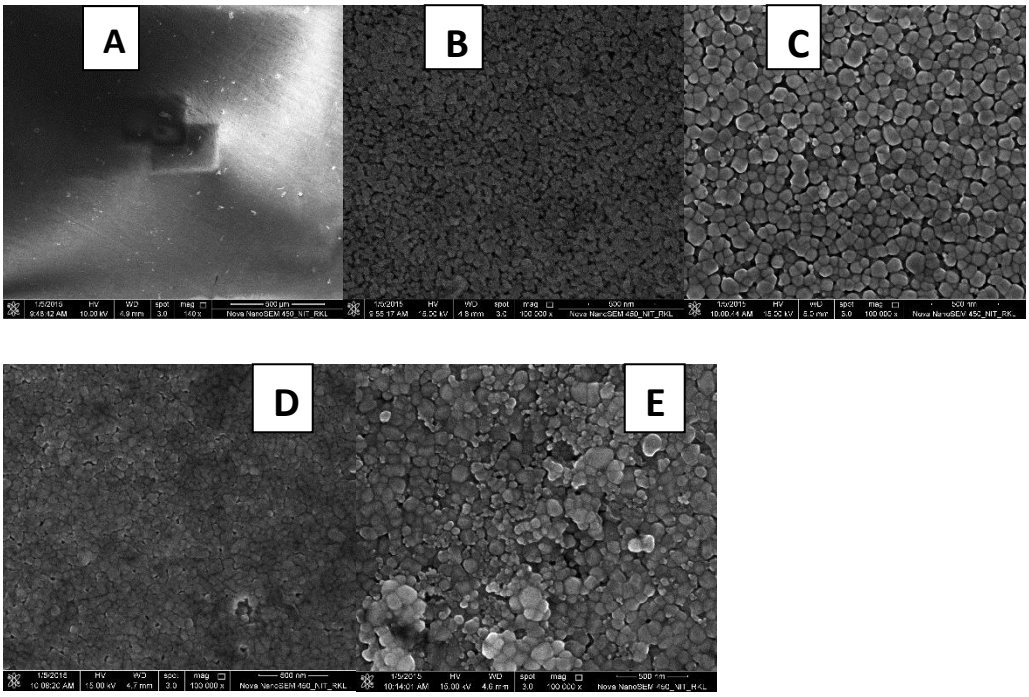

Figure 4.8 FESEM image of Zn TCO (A) Pure glass (B) Zn-TCO Cycle 5 (C) Zn-TCO Cycle 7 (D) Zn-TCO Cycle 10 (E) Zn-TCO Cycle 12

With the increase in number of coatings on glass, the formation of clear particle boundaries was observed. Cycles above 7, the particle boundaries starts to merge together creating tension on the thin film. At cycle 12, there were overgrowth ZnO particles.

4.11 UV reflectance analysis of Zn-TCO

The wavelength range under study was the UV-visible region of electromagnetic spectrum. The calculation details for band gap measurement are shown in ***Appendix A***. From the graphs it can be seen that the band gap of ZnO coated TCO is nearly 3.3 in almost all cases.

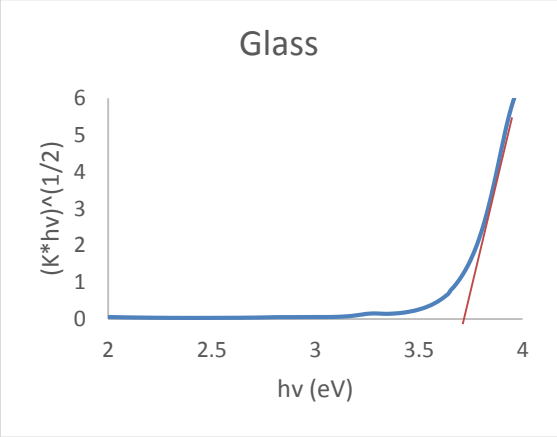

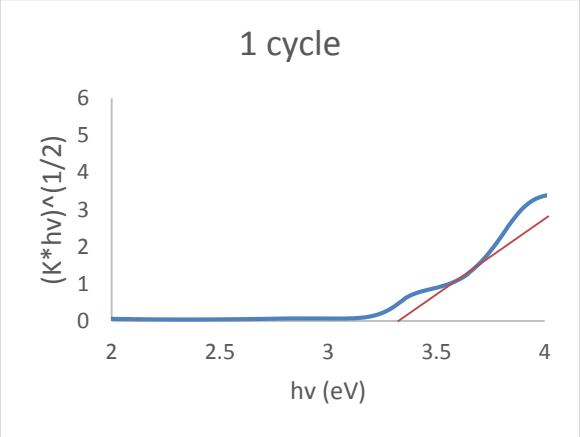

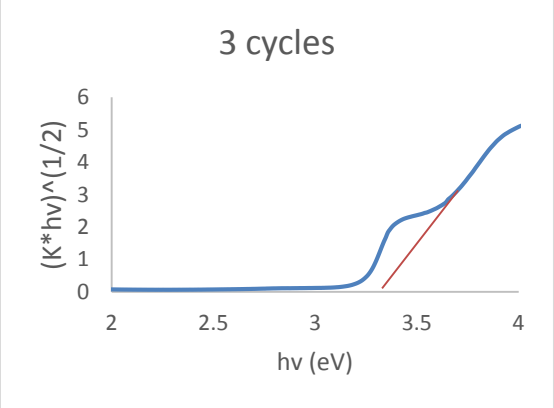

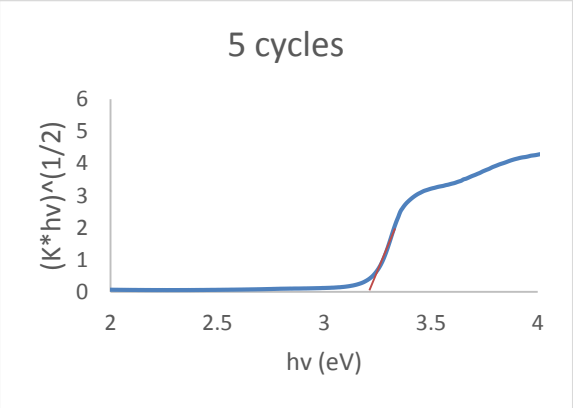

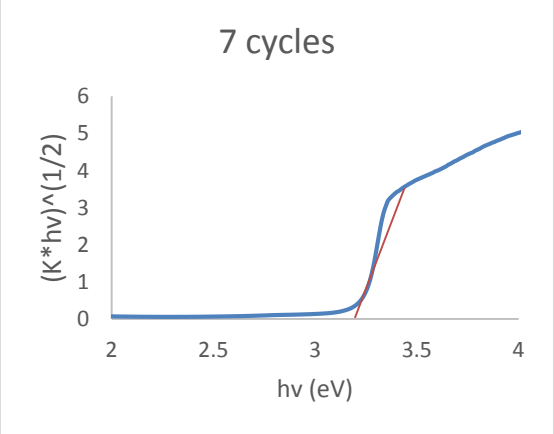

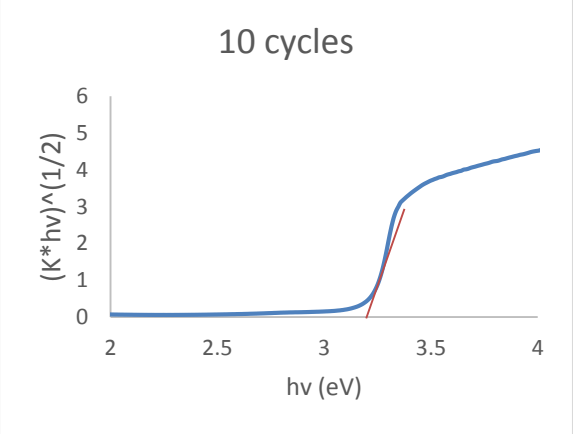

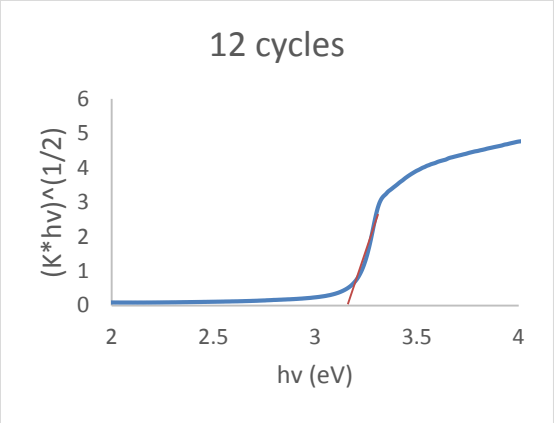

Figure 4.9 Band gap measurement of various cycle of Zn-TCO

4.12 UV transmittance analysis of Zn-TCO

The figure below shows the transmittance percentage of various cycles of Zn-TCO. It can be easily inferred from the graph that the un-coated glass has the maximum transmittance of more than 95% and the transmittance percentage decreases with the increase in number of coatings. There is nearly a decrease of 10% in transmittance in 12 cycles of coating which is the due to the axial growth of ZnO film.

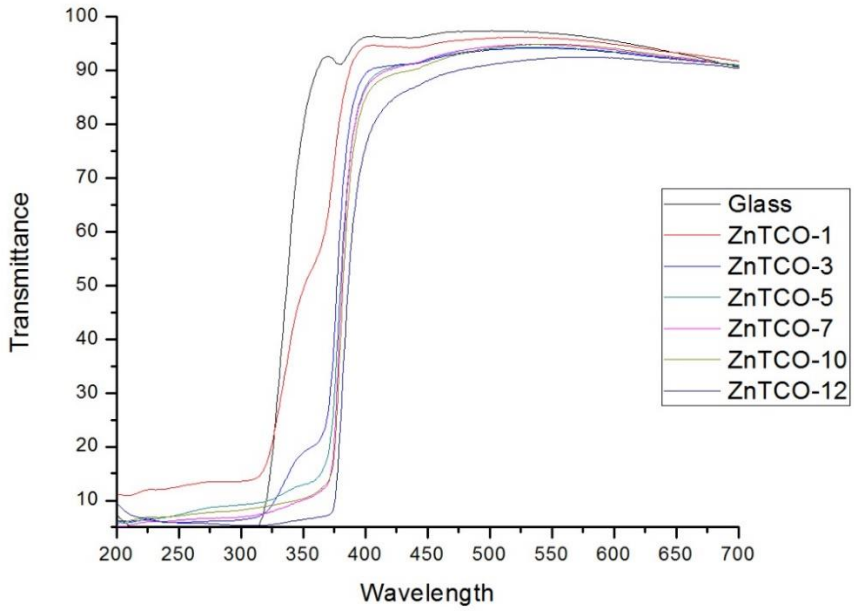

Figure 4.10 UV transmittance values for Zn-TCO

4.13 XRD patterns of Lead (Pb) doped Zn-TCO

The XRD pattern of 1% Pb doped Zn-TCO of various cycles is shown in the **Figure 4.11**. The XRD pattern clearly showed the polycrystalline nature of the ZnO film, whose *c*-axis was oriented normal to the glass substrate. The (002) peak intensity was found at 2Θ equal to 38.

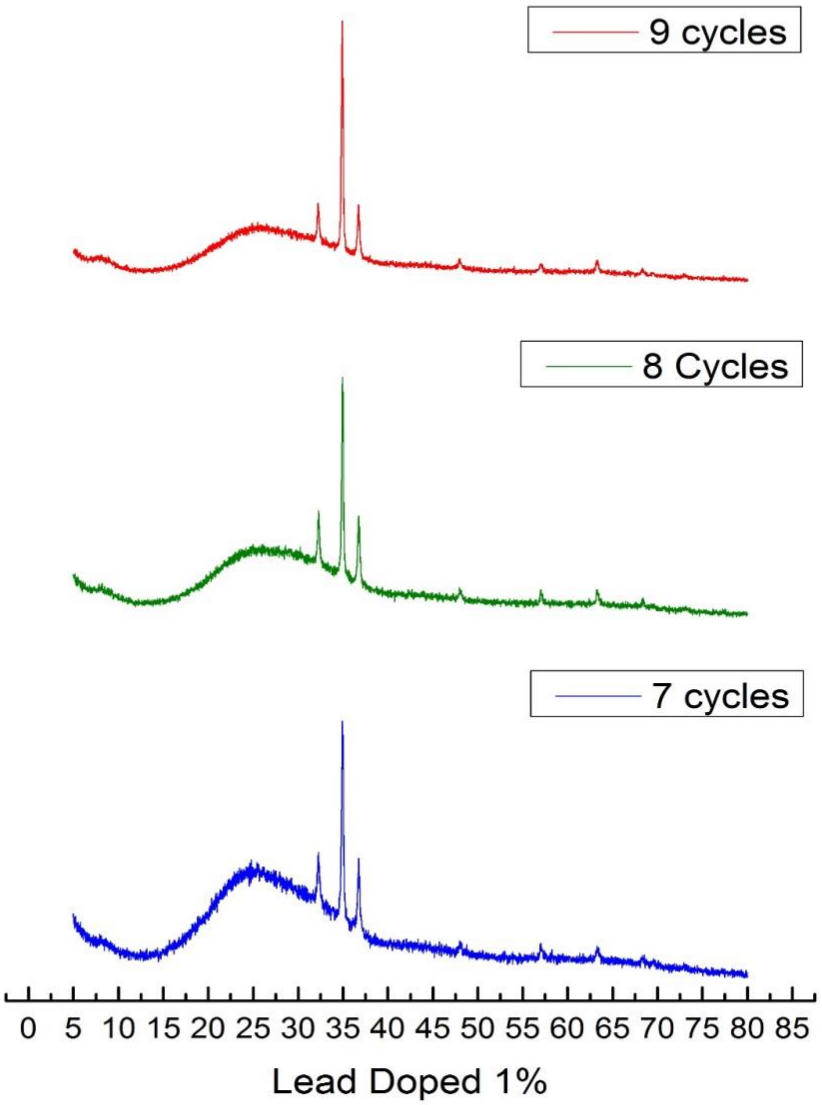

Figure 4.11 XRD patterns of 1% Lead doped coated with various cycles

The XRD pattern of 2% Lead doped is shown in the **figure 4.12**

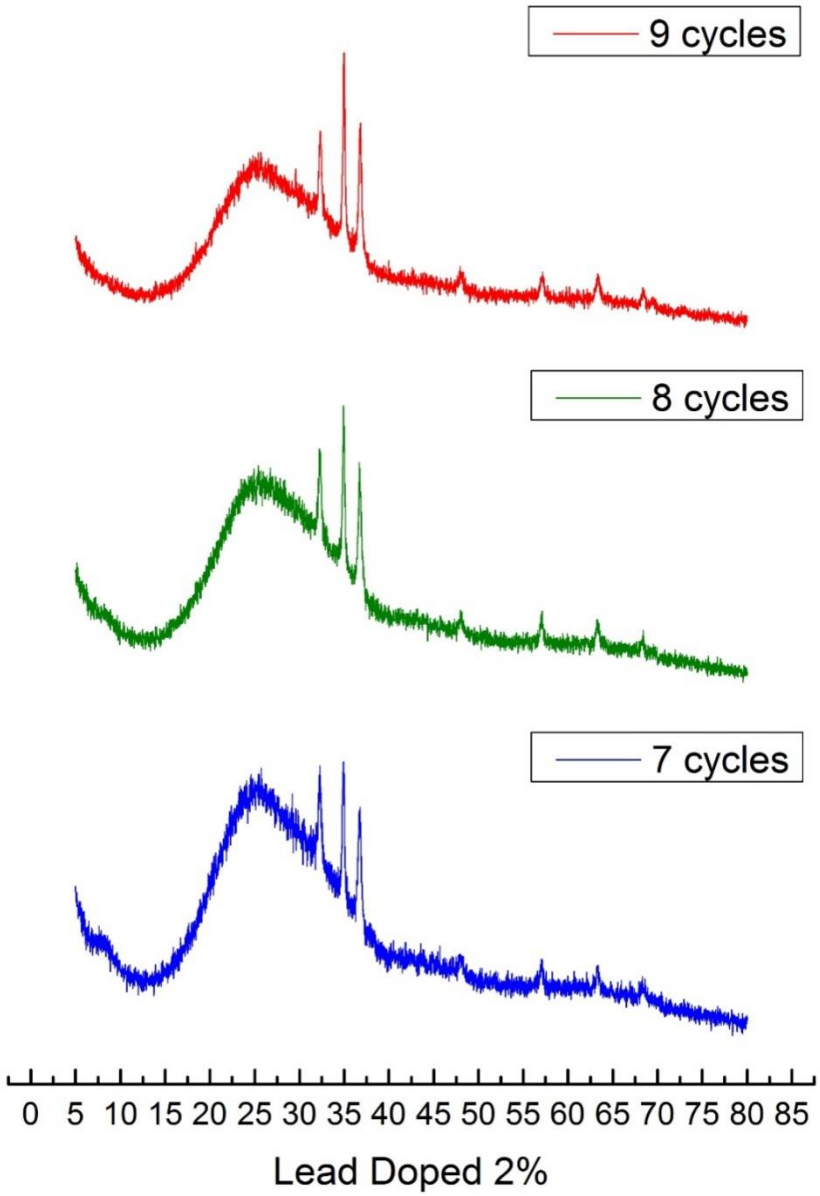

Figure 4.12 PXRD patterns of 2% Lead doped Zn-TCO with various cycles

The crystallinity nature is seen to be better in 1% doped TCOs than the 2% ones. The c-axis growth also increases with the number of cycles.

4.14 UV reflectance analysis of Lead doped Zn-TCO

The wavelength range under study was the UV-visible region of electromagnetic spectrum. The calculation details for band gap measurement are shown in ***Appendix A***. From the graphs it can be seen that the band gap of ZnO coated TCO is nearly 3.3 eV in almost all cases.

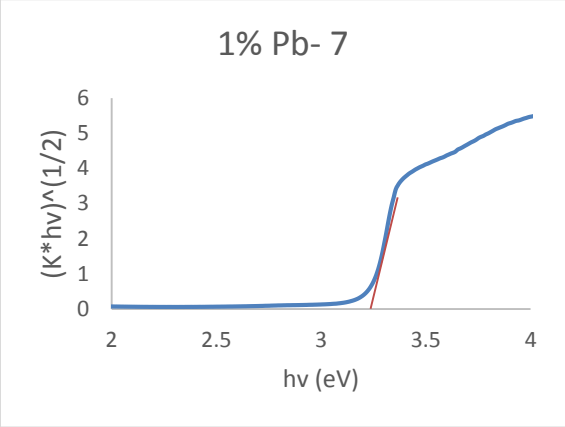

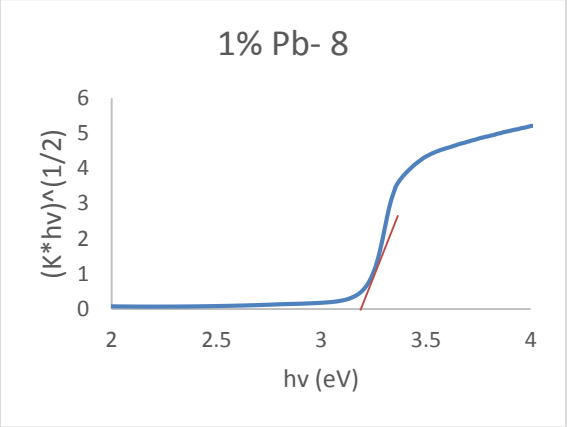

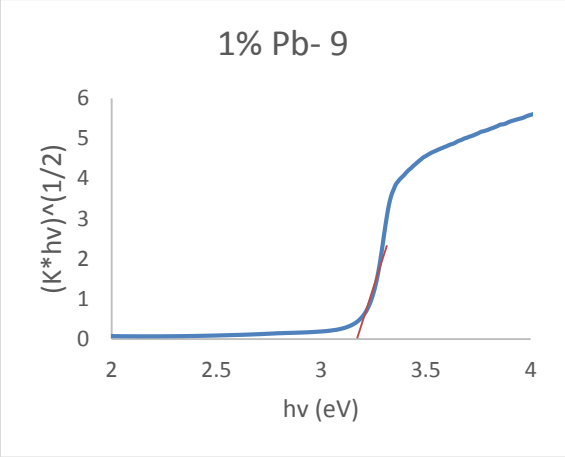

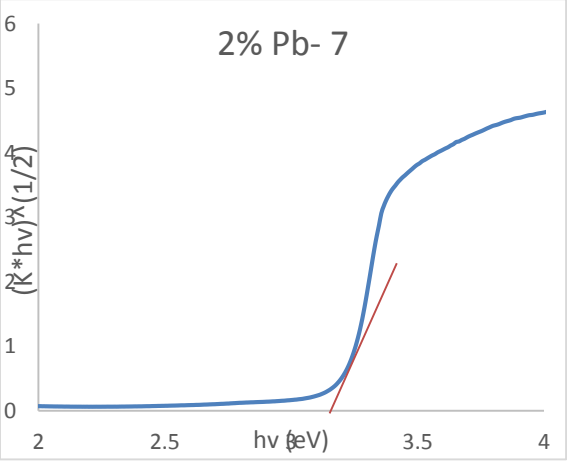

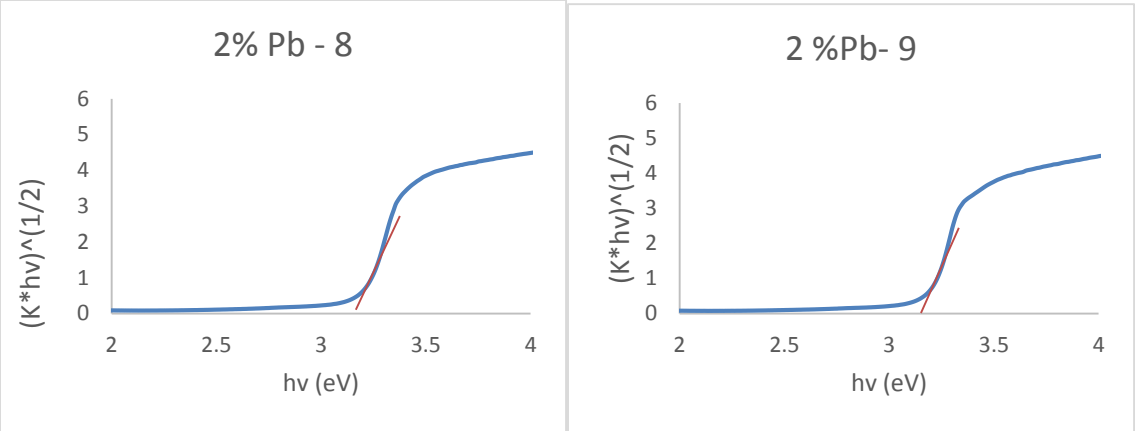

Figure 4.13 Band gap measurement of various lead doped Zn-TCO

4.15 UV transmittance studies of Lead doped Zn-TCO

The transmittance percentage has been plotted against the wavelength in the figure. The transmittance is seen to decrease with the number of cycles of the coatings.

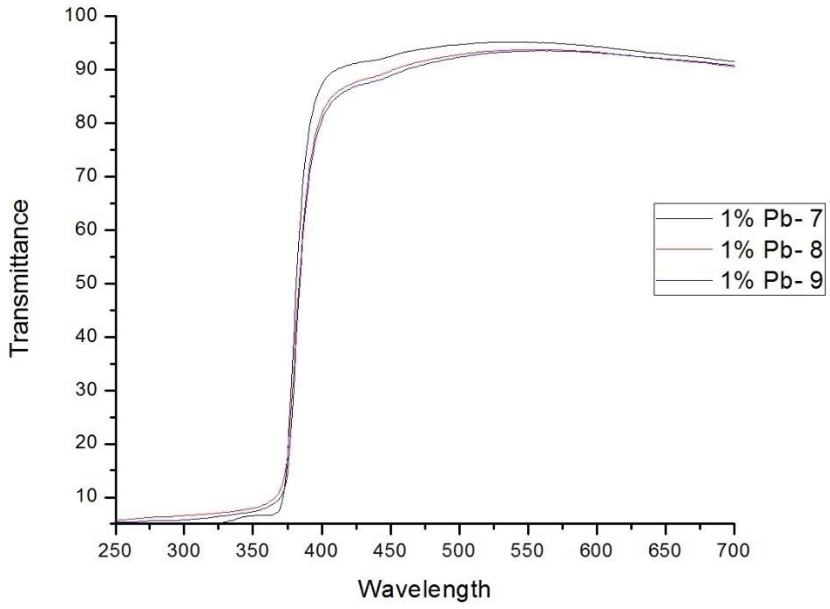

Figure 4.14 Transmittance graph of 1% lead doped Zn-TCO

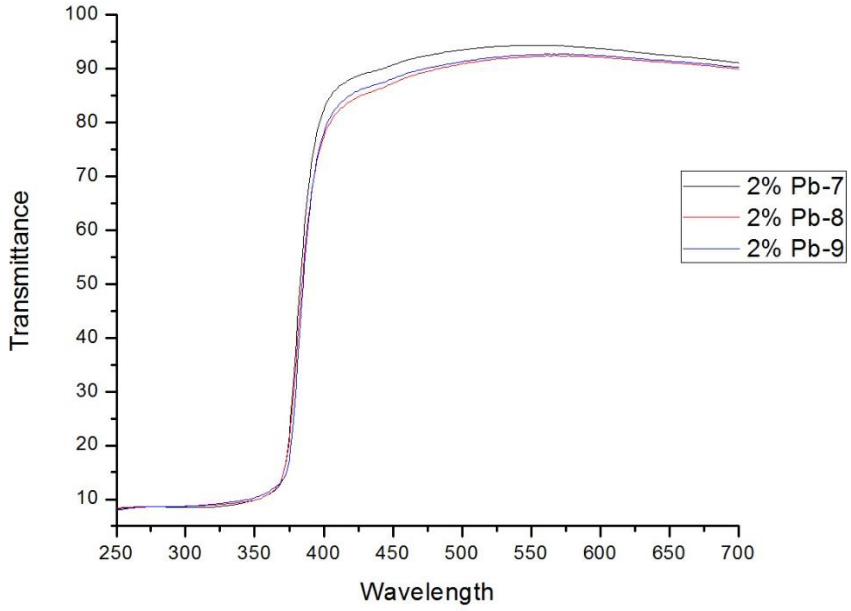

Figure 4.15 Transmittance graph of 2% lead doped Zn-TCO

4.16 XRD patterns of Aluminium doped (Al) Zn-TCO

The XRD patterns of Zn-TCO doped with Aluminium to various percentages are shown in the Figure. The number of cycles in all the cases is 10. The aluminium doped Zn-TCO didn't show much of crystallinity structure at higher percentages of Aluminium.

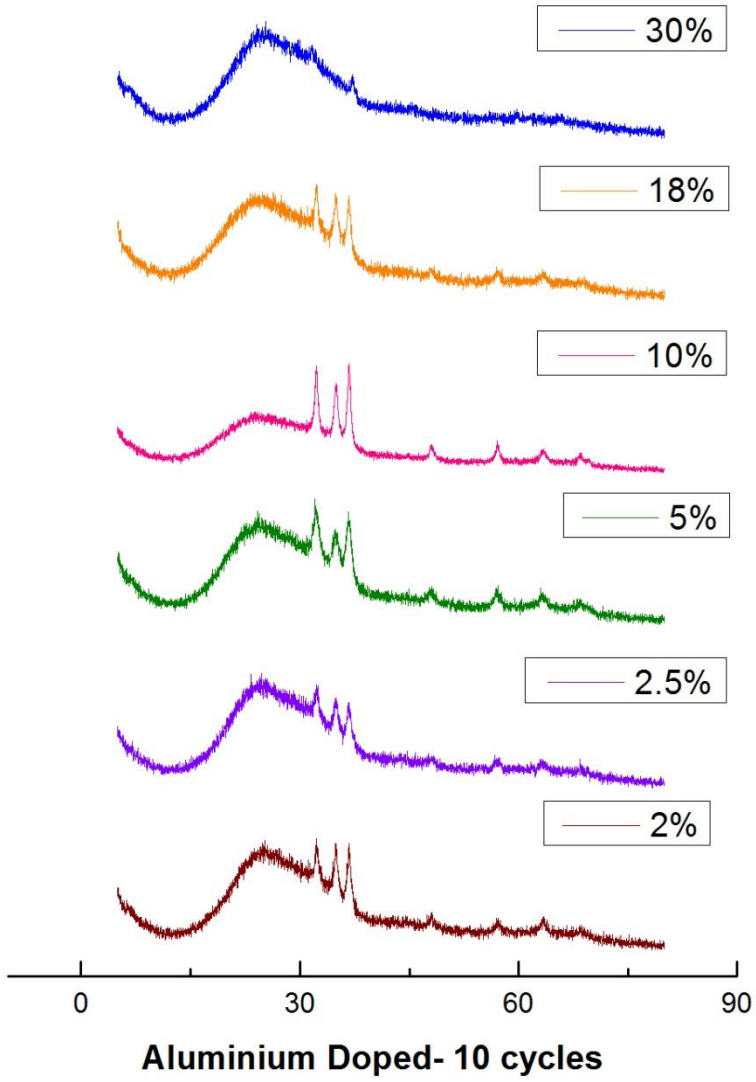

Figure 4.16 XRD patterns of various percentage Aluminium doped Zn-TCO (10 cycles)

4.17 Surface morphology studies of Aluminium doped Zn-TCO

Figure 4.17 shows the SEM image of ZnO:Al thin film with different Aluminium doping concentration. The film was seen to crack at higher percentage of Aluminium. The grain size decreased with increasing Al concentration.

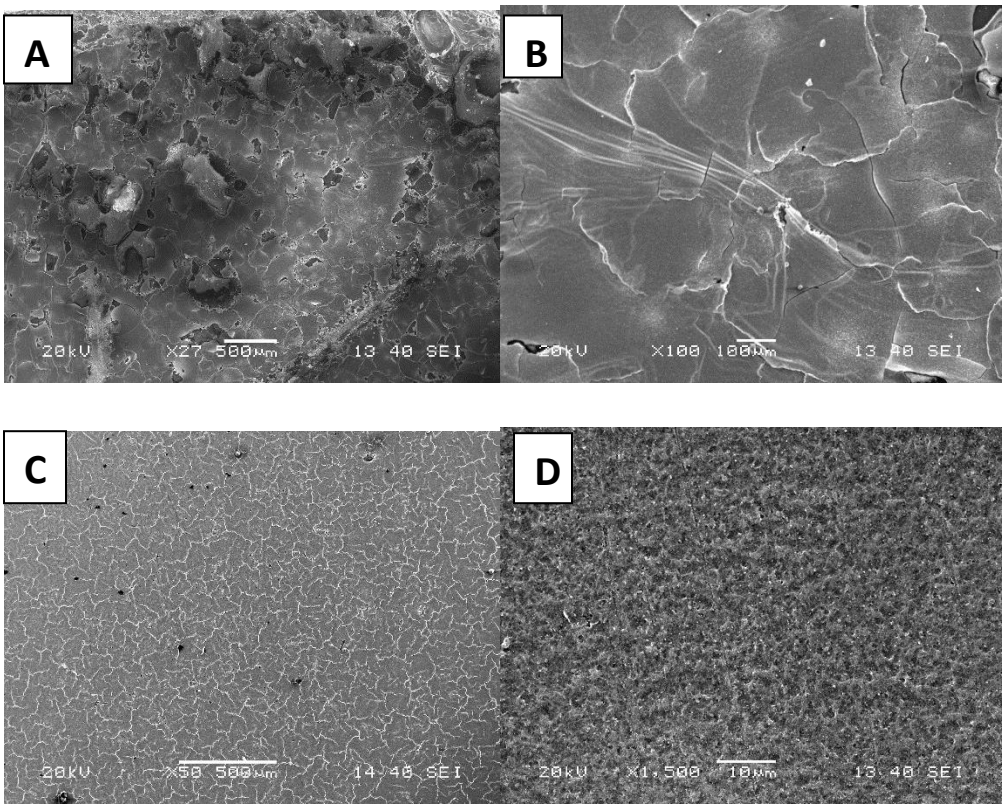

Figure 4.17 SEM image of Aluminium doped Zn-TCO (A) 30% (B) 10% (C) 2% (D) 1%

4.18 UV reflectance studies of Aluminium doped Zn-TCO

The band gap values as calculated from reflectance data is nearly 3.3 eV in all cases except 30% Al.

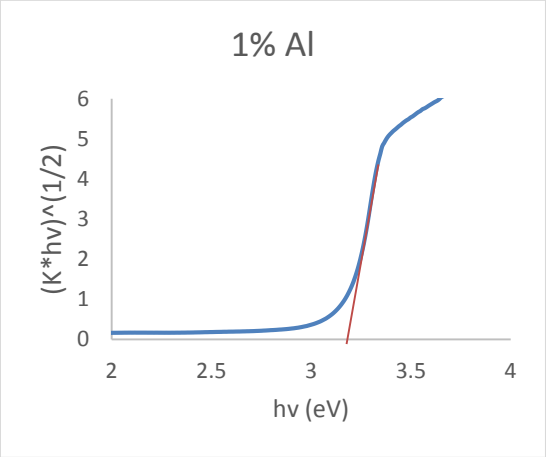

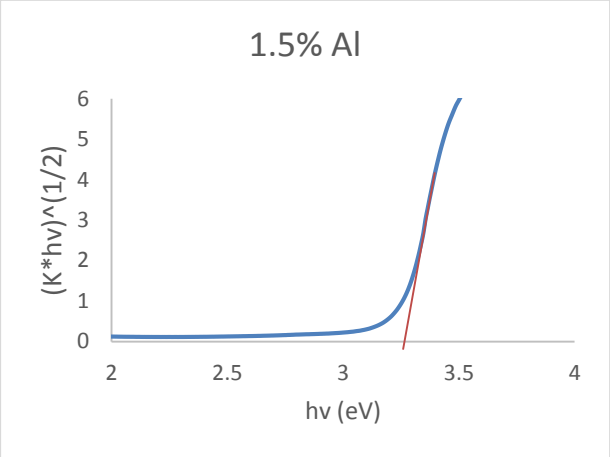

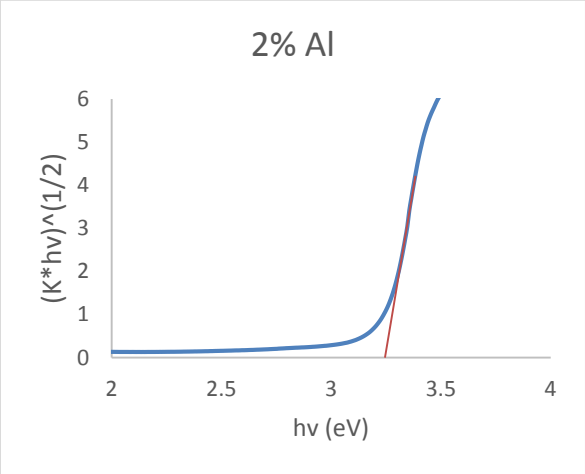

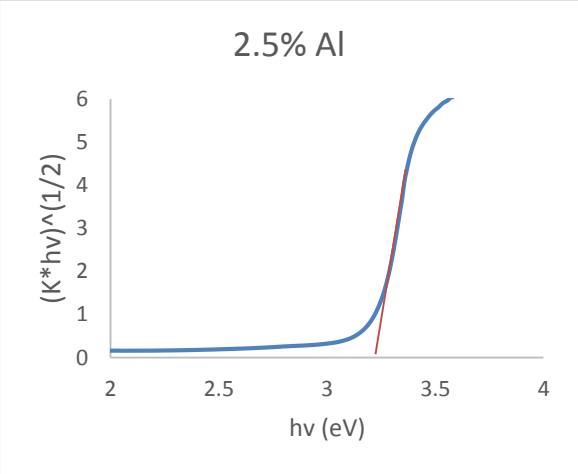

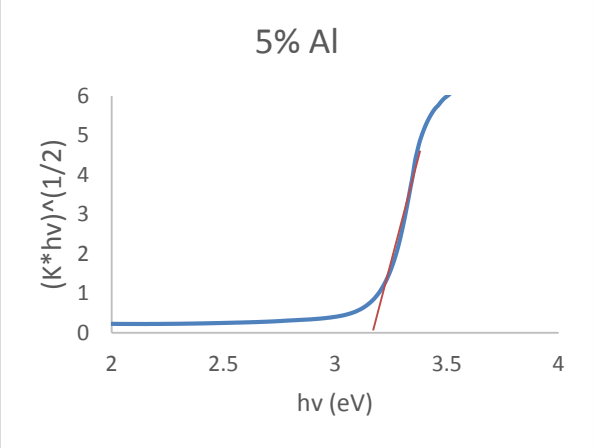

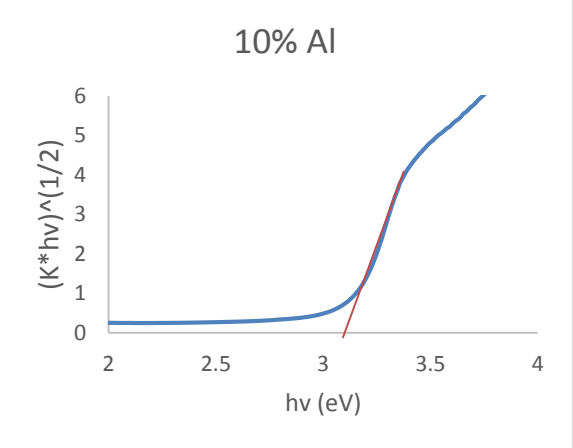

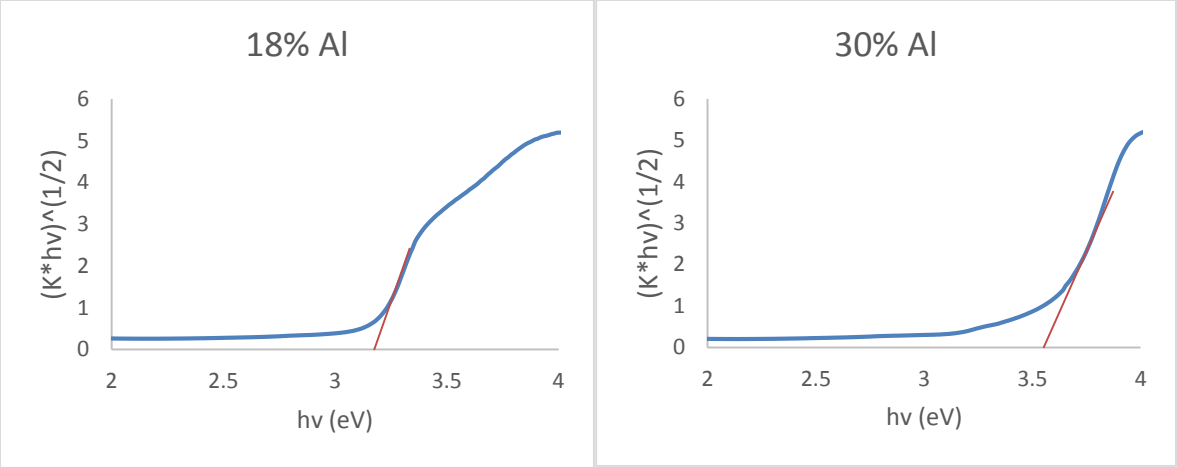

Figure 4.18The band gap measurements of Aluminium doped Zn-TCO to various percentages.

4.19. UV transmittance analysis of Aluminium doped Zn-TCO

The transmittance value decreases with the increase in dopant concentration as seen from the graph. 2% Al shows best transmittance is the desired wavelength region.

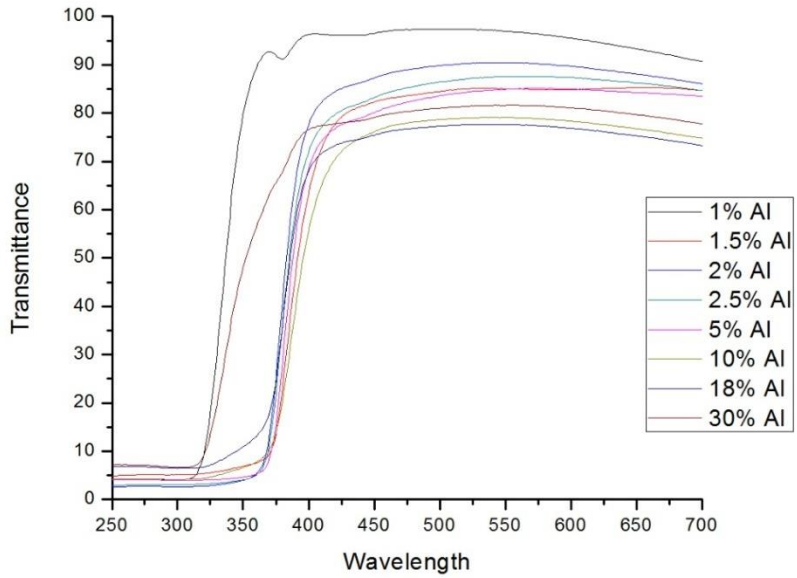

Figure 4.19 UV transmittance studies of Al doped Zn-TCO

4.20 Degradation of Ammonium ion

The degradation profile of Ammonium ion by all the three photo catalysts is shown in the **figure 4.20.**

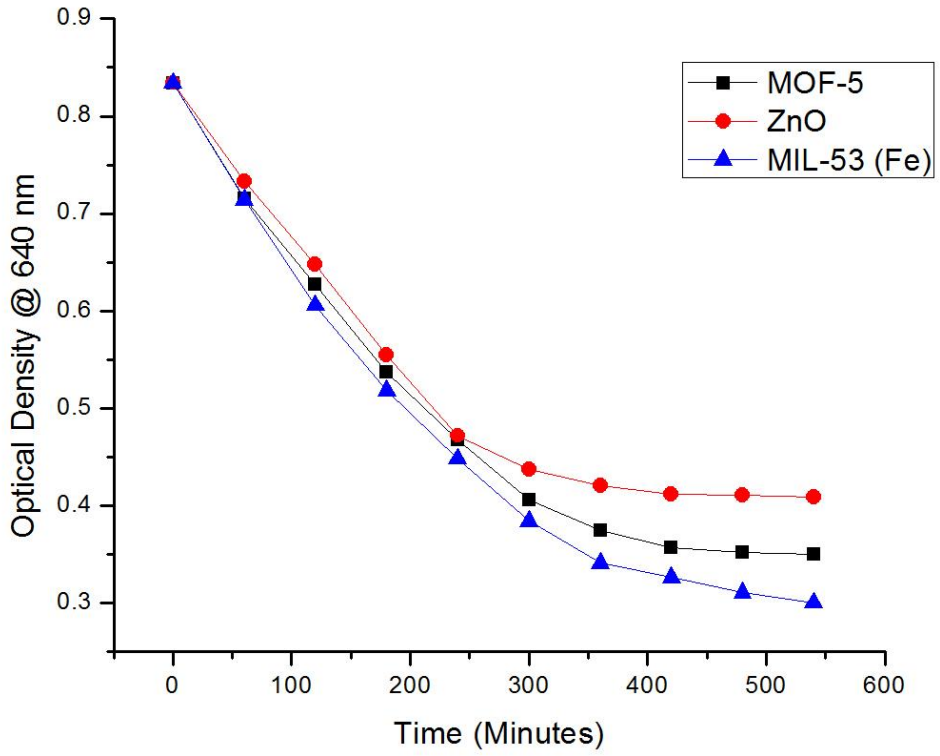

Figure 4.20 Ammonium degradation profile

The percentage degradation in each case is

(a) MOF 5 – 58%

(b) ZnO – 51%

(c) MIL 53 (Fe) – 63%

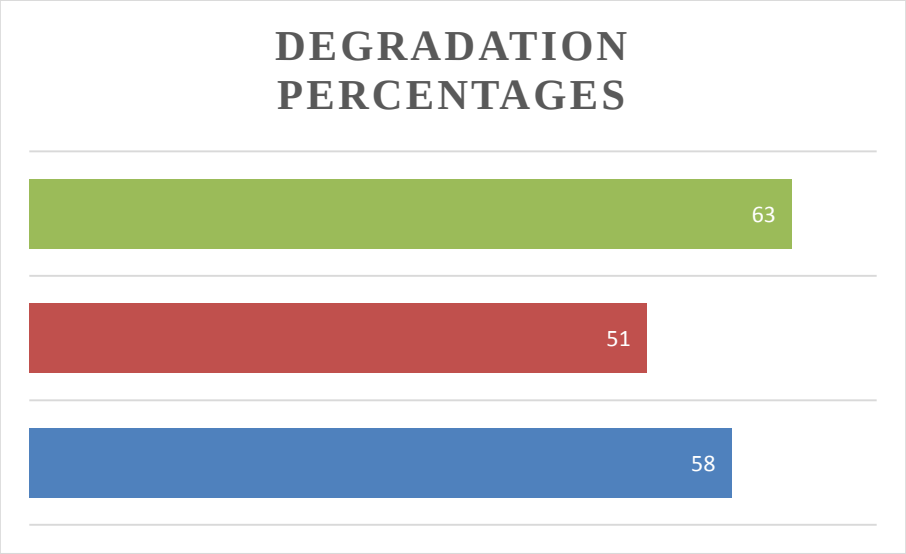

Figure 4.21 Degradation percentages in each case.

The degradation percentage was found to be higher in the cases of metal organic frameworks owing to their high surface, thus increasing the rate of photo catalysis.

The photo catalytic oxidation is activated by the ultra-violet irradiation.

$$ZnO + hv \longrightarrow h^+ + e^-$$

In photo catalytic reactions the positive holes (h^+) and negative electrons (e^-) that are generated play a major role. They participate in the redox reactions and hydroxyl radicals are produced by the decomposition of water. This hydroxyl group facilitates the oxidation of ammonia into N_2.

$$H_2O + h^+ \longrightarrow \cdot OH + H^+$$

$$NH_3 \longrightarrow NH_2 \longrightarrow NH \longrightarrow N_2$$

From the standard graph (Appendix B) the relationship between the optical density and concentration was found out. Hence the concentrations corresponding to the optical density were also known.

The rate constants can be calculated from the graph between ln(C/Co) and time.

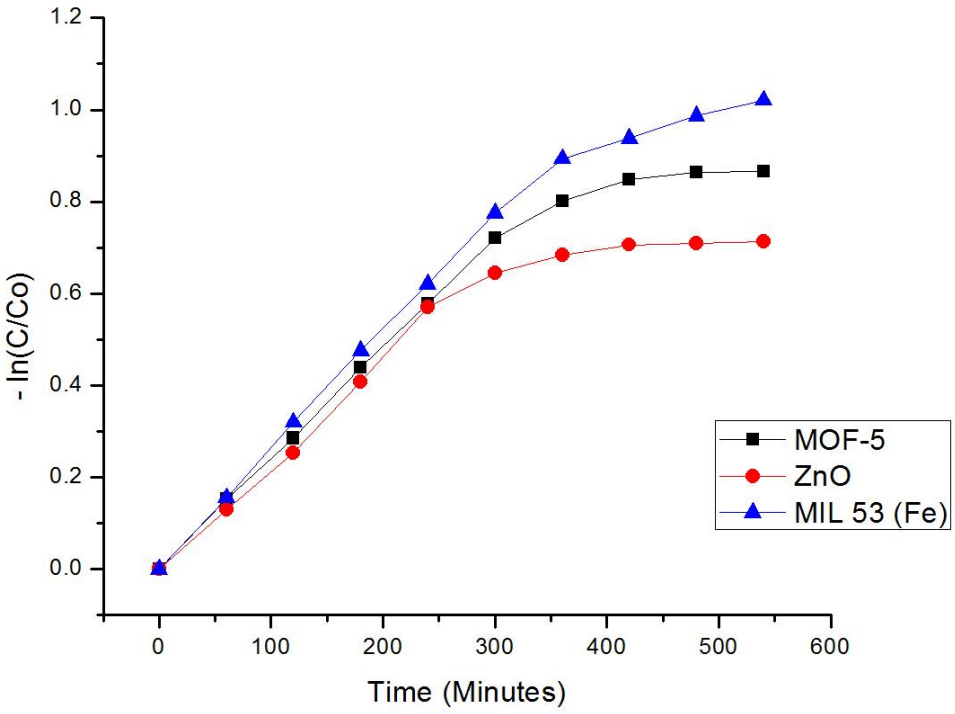

Figure 4.22 Relationship between [-ln(C/Co)] and time

Table 4.1 Ammonia degradation data

Catalyst	Weight of catalyst (mg)	% degradation	Rate constant (min^{-1})
MOF- 5	10	58	0.002
ZnO	30	51	0.0017
MIL-53 (Fe)	10	63	0.0022

It can be concluded that the rate constant is highest for MIL-53 (Fe) and lowest for ZnO.

CHAPTER 5

CONCLUSION AND FUTURE SCOPE

In this work, two contemporary metal organic frameworks (MOFs) i.e. MOF-5 (Zn-BDC) and MIL-53(Fe) (or, Fe-BDC) were synthesized using *microwave synthesis* technique and characterized. Owing to their photo-sensitivity, both the MOFs were used in photo-degradation of ammonia. The results were compared with the performance of a standard photocatalyst *viz*. ZnO. Transparent conducting oxide (TCO) thin films were fabricated by sol-gel and spin coating techniques. MOF films (Zn-BDC) were grown onto TCO. Improvisations were also made in TCO matrix by using Al and Pb as doping agents. The doping percentage as well as the number of cycles of coating was varied so as to get the most suitable TCO. The films were characterized using X-ray diffraction, Scanning electron microscopy, UV-reflectance and UV-transmittance (by spectrophotometer) study. The band gap calculations for the films were measured from the UV-reflectance data which showed the band gap value of nearly 3.2 eV. The performance study of MOFs and ZnO as photocatalyst were carried out in degradation of ammonia. When used directly, MOFs had shown a better degradation percentage (*ca*. 60%) as compared to ZnO and that could be attributed to their very high specific surface area as compared to ZnO. Meanwhile, TCO films of various combinations when tested for their electrical conductivity are met with limited success and further work is going on towards achieving the targeted results.

The work has plenty of future scope.

(a) The fine tuning of zinc based TCO needs to be done so as to achieve reasonable conductivity.

(b) Various other dopants can be used to decrease the resistivity of the films.

(c) Layer by layer synthesis method can also to be used to grow MOFs on the conducting TCO so as to develop a photo electrode capable of degrading water borne pollutants.

(d) Alternatively, electrochemical synthesis of MOF-5 on Zinc plates can be carried out. [*The basic work has already been started. The following is the schematic with reaction mechanism*]

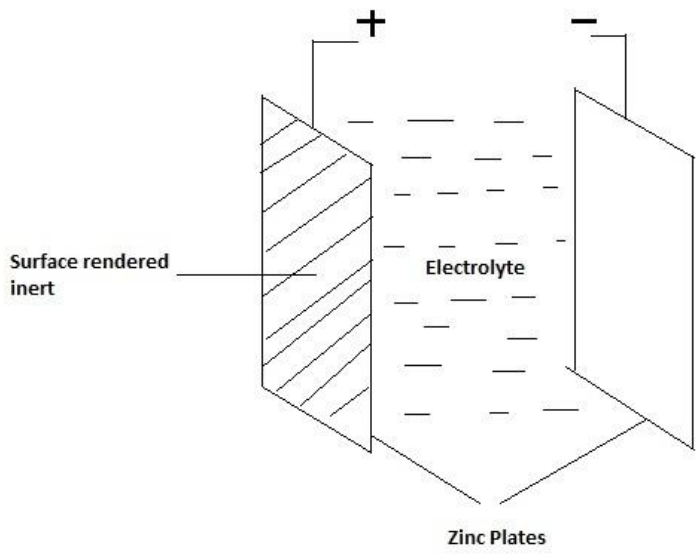

Figure 5.1 Electrochemical synthesis of MOF-5 on Zinc plates

The electrochemical deposition is performed in an electrolytic cell consisting of a power supply, a synthesis electrolyte solution and two electrodes connected to the power source with stainless steel clips.

The electrolyte comprises of Di-Methyl Formamide (DMF), Benzene Di-carboxylate (BDC) and water. Zinc plates are to be used as electrodes.

Cathode: $Zn - 2e^{-} \rightarrow Zn^{2+}$

Anode: $Zn^{2+} + BDC^{2-} \rightarrow ZnBDC$ (MOF-5)

REFERENCES CITED

[1]. Marye Anne Fox and Maria Dulay, "Heterogeneous Photocatalysis", *Chem. Rev.*, **83**, 341-357 (1993).

[2]. Skoulidas, A. I., and Sholl, D. S.,"Self-diffusion and transport diffusion of light gases in metal-organic framework materials assessed using molecular dynamics simulation," *J. Phys. Chem. B*, **109**, 15760-15768 (2005).

[3]. Düren,T., and Snurr,R.Q., "Assessment of Isoreticular Metal-Organic Frameworks for Adsorption Separations: AMolecular Simulation Study of Methane/*n*-Butane Mixtures," *J. Phys. Chem. B*, **108**, 15703-15708 (2004).

[4]. Eddaoudi, M., Li, H., and Yaghi, O. M.," Highly Porous and Stable Metal-Organic Frameworks: Structure, Design and Sorption Properties," *J. Am. Chem. Soc.*, **122**, 1391-1397 (2000).

[5].Wang,Q.M., Shen,D., Bülow,M., Lau,M.L., Deng,S., Fitch,F.R., Lemcoff,N.O., Semanscin,J.,"Metallo-organic molecular sieve for gas separation and purification," *Micropor. Mesopor. Mater.*, **55**, 217-230 (2002).

[6]. Millward, A. R., and Yaghi, O. M.," Metal-Organic Frameworks with Exceptionally High Capacity for Storage of Carbon Dioxide at Room Temperature," *J. Am. Chem. Soc.*, **127**, 17998-17999 (2005).

[7]. Vishnyakov, A., Ravikovitch, P. I., Neimark, A. V., Bülow,M., Wang, Q. M.,"Nanopore structure and sorption properties of Cu-BTC metal-organic framework," *Nano Lett.*, **3**, 713-718 (2003).

[8]. Senkovska, I. and Kaskel, S.," High pressure methane adsorption in the metal-organic frameworks $Cu_3(btc)_2$, $Zn_2(bdc)_2dabco$, and $Cr_3F(H_2O)_2O(bdc)_3$," *Micropor. Mesopor. Mater.*,**112**, 108-115 (2008).

[9].Alaerts, L., Séguin,E., Poelman,H., Thibault-Starzyk,F., Jacobs,P.A., and De Vos,D.E., "Probing the Lewis Acidity and Catalytic Activity of the Metal-Organic Framework $[Cu_3(btc)_2]$ (BTC=Benzene-1,3,5-tricarboxylate),"*Chem. Eur. J.*, **12**, 7353-7363 (2006).

[10]. Rosi, N. L., Eckert, J., Eddaoudi, M., Vodak, D. T., Kim, J., O'Keeffe, M., and Yaghi, O. M.," Hydrogen Storage in Microporous Metal-Organic Frameworks," *Science*, **300**, 1127-1129 (2003).

[11]. Wong-Foy, A. G., Matzger, A. J., and Yaghi, O. M., "Exceptional H_2 Saturation Uptake in Microporous Metal-Organic Frameworks," *J. Am. Chem. Soc.*, **128**, 3494-3495 (2006).

[12]. F. Millange *et al*.,"Effect of the Nature of the Metal on the Breathing Steps in MOFs with Dynamic Frameworks", *Chem. Commun.* (2008) 4732-4734.

[13].M.A. Nasalevich, M. van der Veen, F. Kapteijn and J. Gascon, "Metal–organic frameworks as heterogeneous photocatalysts: advantages and challenges", *CrystEngComm*, **16**, 4919-4926 (2014).

[14]. Jin-Liang Wang, Cheng Wang and Wenbin Lin, "Metal−Organic Frameworks for Light Harvesting and Photocatalysis", *ACS Catal.*, **2**, 2630–2640 (2012).

[15]. Yu-Ri Lee, Jun Kim, and Wha-SeungAhn, "Synthesis of metal-organic frameworks: A mini review", Korean J. Chem. Eng., **9**, 1667-1680 (2013)

[16]. Chandan Dey, Tanay Kundu, Bishnu P. Biswal, Arijit Mallick and Rahul Banerjee, "Crystalline metal-organic frameworks (MOFs):synthesis, structure and function", Acta Crystallographica, B, 2052-5206 (2013)

[17]. Ratheesh Kumar P. M., "SPRAY PYROLYSED ZINC OXIDE THIN FILMS: EFFECTS OF DOPING AND ION BEAM IRRADIATION", Student paper, (2007)

[18]. Andreas Stadler, "Transparent Conducting Oxides—An Up-To-Date Overview", *Materials*, **5**, 661-683 (2012).

[19]. Lamia Znaidi, "Sol–gel-deposited ZnO thin films: A review", Materials Science and Engineering B, **174**, 18–30 (2010).

[20]. Y. Natsume, H. Sakata, "Zinc oxide films prepared by sol-gel spin-coating", Thin Solid Films, **372,** 30-36 (2000).

[21]. Joydip Sengupta, R.K. Sahoo , K.K. Bardhan, C.D. Mukherjee, "Influence of annealing temperature on the structural, topographical and optical properties of sol–gel derived ZnO thin films", Materials Letters, **65**,2572–2574(2011)

[22]. Gil Mo Nam and Myoung Seok Kwon, "Al-doped ZnO via Sol-Gel Spin-coating as a Transparent Conducting Thin Film", Journal of Information Display, **10**, 1598-0316 (2009)

[23]. Gil Mo Nam and Myoung Seok Kwon, "F-Doped ZnO by Sol-Gel Spin-Coating as a Transparent Conducting Thin Film", Electronic Materials Letters, **7**, 127-131 (2011)

[24]. Junwei Li *et al*., "Benzenedicarboxylic acid-assisted synthesis of ZnO micro-hexagons from zinc hydroxide nanostrands and their photoluminescence properties", Applied Physics A, **118 (2)**, 683-690 (2015)

[25]. Gabriela BLĂNIŢĂ et al, "MICROWAVE ASSISTED SYNTHESIS OF MOF-5 AT ATMOSPHERIC PRESSURE", *Rev. Roum. Chim., 56*(6), 583-588 (2011)

[26]. Masoud Zendehzaban et al., "Photocatalytic degradation of ammonia by light expanded clay aggregate (LECA)-coating of TiO_2nanoparticles", Korean J. Chem. Eng., **30(3)**, 574-579 (2013)

[27]. Victor Rosca et al., "Nitrogen Cycle Electrocatalysis", Chem. Rev., **109**, 2209–2244 (2009)

[28]. Feng Zhang et al., "Photocatalytic degradation of ammonia nitrogen with suspended TiO2", IEEE, ICBBE 2009, 1-4 (2009)

APPENDIX

Appendix A: Calculation of Band gap energy from UV reflectance data

The result obtained from UV reflectance spectroscopy contains two main data; wavelength of light incident on the material, Reflectance percentage (R %).

1. The Reflectance percentage (R%) form the experiment was converted to Reflectance (R) by

   $R = (R\ \%) / 100$

2. Followed by the application of Kubelka-Munk transformation of reflectance.

   $K = (1-R)^2 /2R$

Where K is the reflectance transformed according to Kubelka-Munk, R is the reflectance.

3. Construct the relationship curve between $(K\times h\nu)^{1/2} = f(h\nu)$ by plotting $(K\times h\nu)^{1/2}$ on Y axis and f (hν) on X axis.
4. Construct a tangent to the steepest curve to intercept X axis.
5. The interception on the X axis indicates the band gap energy (Eg) of the said material. An example is provided by the graph below.
6. From the graph above, the tangent intercepts X axis at 2.58 eV.

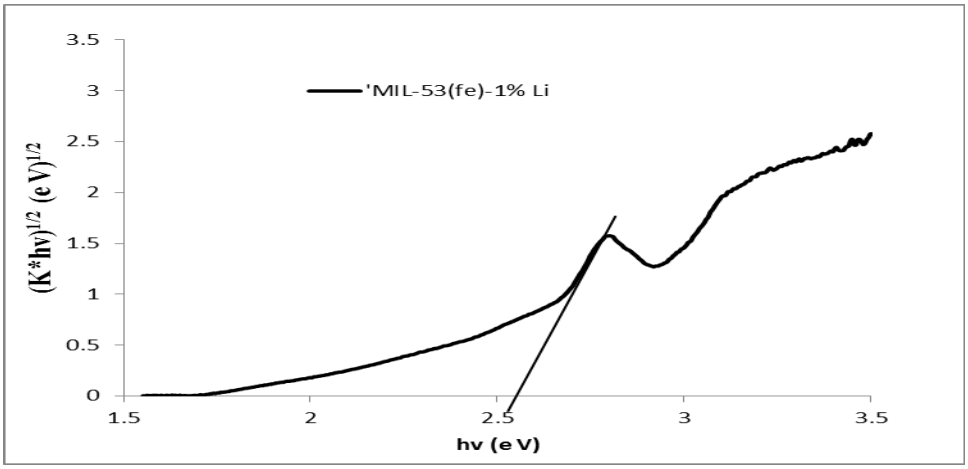

Figure A-1: TAUC plot

Appendix B: Standard curve for estimation of ammonium ion

0.038g of Ammonium chloride solution was taken and dissolved in 100 ml water which is the stock solution. 1 ml the solution is then taken and made upto 100 ml which is the working standard.

Table B-1: Standard curve estimation

Volume of NH_4Cl (ml)	Volume of water (ml)	Phenate method	OD @ 640 nm
0	10	↑	0
2	8	|	0.143
4	6	|	0.282
6	4	|	0.4311
8	2	|	0.5524
10	0	↓	0.6682

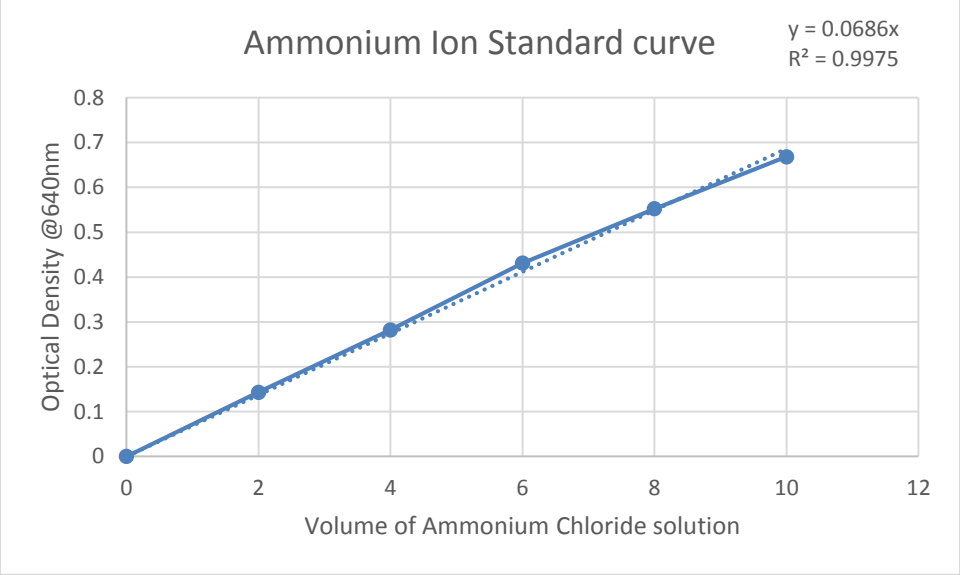

Figure B-1: Ammonium ion standard curve

We can get the relationship equation between optical density and concentration by fitting a linear curve.